NATIONAL AERONAUTIC AND SPACE ADMINISTRATION

ORIGINAL CONTAINS
COLOR ILLUSTRATIONS

TECTONIC EVALUATION OF THE NUBIAN SHIELD OF NORTHEASTERN SUDAN USING THEMATIC MAPPER IMAGERY

Second Interim Report
August 1986

Bechtel

CONTENTS

INTERIM REPORT No. 2

August 1986

CONTENTS

INTERIM REPORT No. 2

August 1986

CONTENTS

INTERIM REPORT No. 2

August 1986

ILLUSTRATIONS

Figure

Plate

CONTENTS

INTERIM REPORT No. 2

August 1986

TABLES

SECTION 1

1.0 EXECUTIVE SUMMARY

Bechtel is nearing completion of a one-year program that uses digitally enhanced Landsat Thematic Mapper (TM) data to compile the first comprehensive regional tectonic map of the Proterozoic Nubian Shield exposed in the northern Red Sea Hills of northeastern Sudan (Figure 1). Prior to this study, the tectonic evolution of the Nubian Shield was not well known (Vail, 1985 and 1983; Garson and Shalaby, 1976; Almond, 1982, 1979, 1978; Almond et al., 1982; Kroner, 1985; Gass, 1982) and was based partly on extrapolation of tectonic events recorded on the Arabian Shield of southwestern Saudi Arabia (Greenwood, et al., 1980). The improved understanding of the geologic setting and distribution of structural and lithologic provinces in the Red Sea Hills resulting from this research is being used to test, verify, and expand existing tectonic models.

Owing to the size, inaccessibility, and harsh, arid climate of the Red Sea Hills, remotely sensed satellite imagery is well suited to analysis of the region. Previously, geologic maps of limited detail and coverage were available for less than half of the area. Thus, fundamental research was required to define and delineate regional structural and lithologic provinces. Recent Landsat Multispectral Scanner (MSS) investigations of the region by Ahmed (1982); Blodget and Brown, 1982; and Bechtel (1983 a,b) documented the ability of satellite imagery to distinguish large Proterozoic shear zones, probable tectonic sutures, ophiolitic assemblages, and multiple periods of orogenesis marked by intrusive activity and fold deformation. As an extension of this earlier work, the current program uses the improved spatial and spectral resolution offered by TM to refine the structural and lithologic provinces and to extend this mapping throughout the northern Red Sea Hills of Sudan. The improved spatial resolution has greatly facilitated the mapping of surface textures, lineaments, contacts, fold belts, and faults. The improved resolution has allowed greater discrimination of bedrock lithologies, particularly in the separation of carbonate from volcaniclastic sediments; the separation of ultramafic, mafic, and ophiolitic complexes; the separation of amphibolite-grade from low-grade

metamorphic rocks, and the resolution of multiple-phase felsic intrusions accompanied by contact metamorphism, hydrothermal alteration, and emplacement of dikes.

The Proterozoic Shield of the Red Sea Hills is exposed over an area of approximately 350,000 square kilometers. Of this region, we selected an area of approximately 125,000 square kilometers of the northern most Red Sea Hills which contains the greatest amount of available geologic data for a preliminary study using Landsat TM imagery. This region borders Egypt, where the Proterozoic basement is relatively well mapped and known ophiolite belts and tectonic sutures extend southward into northern Sudan.

The status of significant objectives of this study are as follows:

- Review of pertinent published and unpublished geologic literature and maps of the northern Red Sea Hills to establish the geologic framework of the region: completed.
- Processing of TM imagery for optimal base-map enhancements; preparation of photo mosaics of enhanced images to serve as base maps for compilation of geologic information: completed.
- Interpretation of TM imagery from photo mosaics and on-screen to define and delineate structural and lithologic provinces: basic interpretations completed; detailed interpretation of problem areas continuing.
- Compilation of geologic information (petrologic, and radiometric data) from the literature review onto base-map overlays: continuing in parallel with detailed interpretation of problem areas.
- Field reconnaissance to establish ground verification for the mapped lithologic and structural provinces: political instability of Sudan prevents completion of the field program at this time.
- Evaluation of the tectonic evolution of the Nubian Shield based on the image interpretation and the compiled tectonic maps: continuing.

For this interim report, photographic images, detailed geologic and generalized tectonic maps, and the accompanying analysis of Scene 172, 45 (Figure 1, Location Map) are presented because they encompass most of the significant elements of the stratigraphic, structural, and tectonic interpretation and history of the Nubian Shield that are emerging from this study. With regard to structure and to lithologic delineation, this is the most complicated scene. In this scene we see good evidence for Proterozoic accretion of oceanic island-arc terranes along significant crustal sutures. Extensions of major tectonic features across the Red Sea rift from the Arabian Shield are readily delineated. It is an excellent scene for demonstrating that the use of TM data yields vast improvements in the understanding of structural, magmatic, and tectonic interpretation and history over what is available in the literature. Specifically, improvements have been made in the more precise resolution of lithologic contacts, faults locations and extents, the regional distribution of specific rock types including metamorphic grades, and the resulting regionalization of major lithotectonic elements.

SECTION 2

2.0 INTRODUCTION

2.1 Previous Work With Landsat Imagery in Arabian-Nubian Shield

Several preliminary Landsat MSS investigations have been conducted over parts of the Arabian and Nubian Proterozoic Shields. Blodget and Brown (1982) used digitally processed winter and summer MSS imagery to aid geologic mapping of regional structure and lithology over portions of the Arabian Shield of southwestern Saudi Arabia. Ahmed (1983) used digitally processed single-band black and white MSS imagery to map lineaments over 400,000 square kilometers of northeastern Sudan. He subsequently explored the correlation of known mineralization in the Proterozoic basement with major lineaments and intersecting lineaments. Almond (1982) used MSS imagery to study lineaments in the Red Sea Hills as an aid in tectonic interpretation.

More recently, Bechtel (1983a,b) used digitally processed winter and summer MSS imagery to map Proterozoic lithology and structure in the Red Sea Hills of Sudan and on the Arabian peninsula. A variety of enhanced images were used to supplement and refine existing geologic maps as well as to produce new maps in areas of sparse geologic information. The improved geologic maps were used to locate favorable targets of potential mineralization and to assist in developing an exploration strategy for the region. Winter imagery with low sun-angle illumination provided the greatest amount of structural information, while the summer imagery with high sun-angle illumination was most useful for determining the spectral characteristics of lithology. In the arid, sparsely vegetated Red Sea Hills both images contributed useful structural and lithologic information. Structural features were enhanced using two-dimensional Fourier analysis, directional filter kernels, and contrast-stretched raw spectral bands and color composite images. Lithology was interpreted from contrast-stretched false-color composites of principal component bands, ratioed bands, and raw spectral bands.

Each of these studies demonstrated the feasibility of using Landsat imagery as a valuable mapping tool in the arid, sparsely vegetated areas of northeastern Sudan and southwestern Saudi Arabia. Landsat studies in the Red Sea Hills by Bechtel (1983a) concluded that Landsat MSS imagery could be used to: (1) discriminate, in places, basement rocks of different metamorphic grade (i.e., amphibolite-granulite grade from greenschist grade from relatively unmetamorphosed rocks); (2) discriminate ultramafic and mafic complexes and metamorphosed basement; (3) detect major Proterozoic shear zones, faults, lineaments, and fold belts; (4) discriminate felsic plutons of different age and separate them from surrounding basement; (5) separate basalt flows for different periods of extrusion based on their iron-content or degree of surface weathering; and (6) identify large areas of gossan and laterite. The spectral and spatial resolution of MSS, however, were not adequate to accurately map many lithologic contacts, to differentiate specific lithologies of felsic and ultramafic rocks, recognize non-limonitic hydrothermal alteration, or to differentiate carbonate from volcaniclastic basement lithologies.

2.2 Landsat Thematic Mapper Data

Major limitations of Landsat MSS imagery for geologic applications result from the coarse spatial resolution and limited spectral coverage (0.5 - 1.1 microns) of this sensor which does not extend into regions of the spectrum most useful for characterizing the spectral properties of geologic surface materials. The Landsat TM overcomes some of the limitations of the MSS sensor because of its improved spatial resolution and extended spectral coverage (band 5 at 1.55 - 1.75 microns and band 7 at 2.08 - 2.35 microns). The short-wavelength infrared region between 1 and 2.5 microns contains both broad-band and narrow-band spectral features that are diagnostic of mineral composition. Prior to the availability of TM spectral-band data, geologic studies using the MSS spectral bands found that limonitic hydrothermally altered rocks and limonitic unaltered rocks were not separable and non-limonitic hydrothermally altered rocks were not detectable (Abrams et al., 1977, 1983, Podwysocki et al., 1983).

2.3 Significance of the Investigation

The tectonic maps generated during this study will provide the foundation for subsequent geologic investigations in the northern Red Sea Hills and surrounding region. The maps are derived from interpretation of Landsat TM imagery complemented by results from earlier Landsat MSS investigations of the region and existing available literature. The earlier MSS studies (Bechtel, 1983a,b) provided the regional lithologic and structural framework for the current TM study. Interpretation of the enhanced TM imagery has verified, refined, and extended the earlier MSS results and documents the relative capabilities of the two systems for regional geologic mapping.

Several reconnaissance maps of portions of the northern Red Sea hills have been published by various authors and agencies. These include work performed by Sudanese, American, Egyptian, German, English and French geologists. Although stratigraphic terminology and lithologic contacts vary greatly from region to region, gross similarity in basic map units is present. The regional perspective and improved spectral and spatial resolution offered by the TM has permitted stratigraphic and structural correlation between maps generated by these various authors.

Interpretation of the generated tectonic maps is greatly expanding current tectonic models proposed for evolution of the Nubian and Arabian Shields. Tectonic evolution of the Nubian Shield previously was not well known and was based partly on the correlation with, and extrapolation of, tectonic events recorded on the Arabian Shield. The improved understanding of the geologic setting and distribution of structural and lithologic provinces in the Red Sea Hills resulting from this study are not only improving our knowledge of the evolutionary growth of the Nubian Shield, but are also allowing improved correlation with tectonic events recorded on the Arabian Shield of Saudi Arabia, the Mozambique Mobile Belt of Africa, and the Nubian Shield of southern Egypt.

SECTION 3

3.0 GENERAL GEOLOGY

3.1 Sudan

The Republic of the Sudan is the largest country in Africa, occupying nearly one million square miles. Owing to its vastness and inaccessibility, detailed geologic mapping is difficult, and reconnaissance surveys have been the primary source of geologic information. Digital image processing of Landsat imagery can contribute to this program by providing regional lithologic and structural information in those areas where access is difficult and existing information is sparse. The rocks in Sudan are divided into the Proterozoic igneous and metamorphic rocks of the Nubian Shield and younger Phanerozoic cover series (Vail, 1978 A, Whiteman, 1971). Figure 2 presents a generalized lithologic map (Almond, 1978).

3.1.1 Proterozoic Continental Shield

Proterozoic rocks (600 million years to at least 2 billion years old) of the Nubian Continental Shield underlie nearly all of the Sudan (Garson and Shalaby, 1976; Neary, 1978). These rocks are exposed over 49 percent of the Sudan (Ahmed, 1983). They are divided into the stable continental shield complex in the southwest and the continental margin complex in the northeast (the geosyncline complex of Garson and Shalaby, 1976). The Red Sea Hills is part of this Proterozoic continental margin complex. The stable continental shield consists primarily of granites and gneisses. The continental margin complex consists of deformed schists and gneisses intruded by granitic plutons from 900 to 30 million years ago. Scattered ultramafic complexes, representing Proterozoic oceanic crust, are also present along deep crustal sutures. The continental margin complex is believed to have been involved in several continental rifts and collisions during the last 2 billion years (Garson and Shalaby, 1976; Neary, 1978). The continental margin complex in Sudan consists of accreted arc terranes and is the northern extension of the Mozambique mobile belt, the Proterozoic plate margin in southern and eastern Africa (Almond, 1978; Dawoud, 1982; Hepworth, 1979). Calc-alkaline island

arc plutonism and volcanism during the Kibaran orogeny (820 to 900 million years ago) and the Pan-African orogeny (Ca. 530 to 780 million years ago) was widespread along the northern continental margin. (Gass, 1982; Greiling, et al., 1984; Almond, 1982; Fleck, et al., 1976; Kroner, 1979; Sillitoe, 1979). Post-orogenic intrusives, including ring complexes, became increasingly alkaline in composition as the Proterozoic continental margin became "cratonized", or converted to continental crust (Harris, 1982; Bentor, 1984).

3.1.2 Phanerozoic Cover

Half of the Sudan is covered by Phanerozoic (less than 600 million years old) sedimentary and volcanic rocks which rest unconformably on the Proterozoic Arabian-Nubian continental shield (Figure 2). The most extensive cover rocks are the Cretaceous (140 to 65 million years ago) Nubian Sandstone in northwestern Sudan and the Quaternary (less than 2 million years old) alluvial deposits in central and southeastern Sudan. The Nubian Sandstone consists of red quartzose sandstone, mudstone and conglomerate which accumulated in freshwater lakes and on alluvial fans (Vail, 1978; Whiteman, 1971). Cenozoic (less than 65 million years old) marine sediments are present in a strip bordering the Red Sea. Cenozoic volcanic rocks are present in several areas and consist primarily of flood basalts and intrusive plugs. The Phanerozoic sedimentary and volcanic units have not been extensively deformed or metamorphosed (Vail, 1978a).

3.2 Red Sea Hills

The Red Sea Hills are an uplifted and eroded exposure of the Proterozoic continental margin complex in northeastern Sudan (Figure 2). The age, lithology and probable tectonic setting of the principal stratigraphic units are described in Section 5 and in other sources. Vail, 1979 and Ahmed, 1979. The rocks range in age from the Proterozoic to the Cenozoic and include metamorphosed basement rocks, plutons and unmetamorphosed sedimentary and volcanic rocks.

The Proterozoic basement has been stratigraphically divided into the Kashebib, Nafirdeib, and Awat Series (Gass, 1955; Kabesh, 1962; Vail, 1978; Whiteman, 1971). The basal Kashebib Group is metamorphosed to amphibolite facies. It it not clear to us whether in the Red Sea Hills these rocks represent Nafirdeib series rocks with higher metamorphic grade or small pre-Nafirdeib cratonic blocks. The Nafirdeib series is greenschist to amphibolite facies island arc volcanics and sediments. Both units are extensively deformed, whereas the Awat Group is relatively unmetamorphosed and undeformed.

Large plutons of the Batholithic Granite Series intruded the Nafirdeib rocks, and ultramafic rocks were emplaced along faults. The ultramafic rocks include lithologies characteristic of ophiolite assemblages and are believed to be the western continuation of ophiolite belts found in Saudi Arabia (Garson and Shalaby, 1976).

The Batholithic Granite is thought to have been emplaced during late Proterozoic island arc plutonism ca. 900 to 600 million years ago.

Mafic to felsic plutons and ring complexes of the Younger Granite Complex intruded the Proterozoic rocks during the Pan-African Orogeny 400 to 630 million years ago, and in some regions of the Red Sea Hills occupy over half of the exposed surface area. There is disagreement in the literature over the time span that the "Young Granites" encompass. Older "Young Granites" are calc-alkaline and geochemically (El Nadi, 1984) similar to the batholithic granites. Younger "Young Granites" are alkaline in composition, typical of intra-cratonic plutonism (Sillitoe, 1979). Cross-cutting plutons, dikes and ring complexes suggest multiple intrusive phases for many of the Young Granites. This is supported by radiometric age dates which range from 780 to 121 million years old. The Young Granites are subvolcanic, aluminous, and bimodal granitic-gabbroic. The are commonly oval to circular; ring structures are also common. The Asoteriba volcanics, which are contemporaneous with the Batholithic Granites, are 600-700 m.y. (Neary et al., 1976; Cavanagh, 1979).

Cretaceous and Cenozoic sedimentary and volcanic rocks locally cover the older basement and intrusive rocks. These include the eroded remnants of the Nubian Sandstone, post-Nubian sandstone flood basalts and trachytes and the marine deposits along the Red Sea coast. Wind-blown sand, alluvium and colluvium are present along drainages and on slopes, and locally obscure large areas of bedrock.

SECTION 4

4.0 DIGITAL IMAGE ENHANCEMENT

4.1 False-color Composite and Additional Enhancements for Base Map

Statistical techniques for principal-components analysis in remote sensing are well documented (e.g., Merembeck et al., 1977; Sheffield, 1985; Hord, 1982; Chavez et al., 1984; Taylor, 1974; Podwysocki et al., 1977; Blodget et al., 1978). Our base map color combination, while not intended to bring out all the details of each image, was selected to distinguish among major lithologic units and structural features present in the study area. From Gabert's map (1960), previous related Landsat MSS studies (Blodget et al., 1978; Bechtel, 1983 A and B), and literature discussions of geologic features within the area of interest (e.g.. Vail, 1985, 1983, 1979, 1978; Almond, 1978, 1979, 1982; El Nadi, 1984; al Shanti and Roobol, 1979), the major features that required discrimination were:

(1) ophiolites
(2) metasediments
(3) metavolcanics
(4) limestones
(5) granitic intrusions of different ages and compositions
(6) structural features, with particular emphasis on zones containing major sutures and offset along faults

Using scene 173, 45, which was the first tape received from NASA, we examined the entirety of the structurally interesting Quad 2. A general statistics study demonstrated that data in the spectral bands of TM were highly correlated, as shown in Table 4-1.

Table 4-1: Interband Statistics, 172,45 Q2

Band 1	Band 2	Band 3	Band 4	Band 5	Band 7
Lower Triangle Cov. Matrix					
1					
1273.798					
2					
784.597	500.350				
3					
1176.571	754.985	1153.580			
4					
909.839	585.449	896.292	704.951		
5					
1581.228	1011.041	1551.547	1228.510	2276.723	
6					
1023.014	653.513	1002.807	795.009	1473.827	976.054
Mean Vector:					
107.996	52.806	73.422	57.135	115.436	74.305
Min. Vector:					
.000					
Max. Vector:					
251.000					
Std. Dev:					
35.690					
Eigen Values:					
.967	-.024	-.005	-.002	-.000	-.000
Eigen Vectors:					
1					
-.424	-.269	-.411	-.322	-.577	-.374
2					
-.587	-.275	-.294	-.099	.552	.420
3					
.655	-.151	-.544	-.450	.103	.192
4					
.043	-.045	-.075	-.038	.586	-.803
5					
.166	-.467	-.348	.790	-.078	-.027
7					
.125	-.779	-.565	-.237	-.003	.077
E_1	E_2	E_3	E_4	E_5	E_7

Table 4-1, continued

Correlation Matrix

	1	2	3	4	5	7
1	-					
2	.983	-				
3	.971	.994	-			
4	.960	.986	.994	-		
5	.929	.947	.951	.969	-	
7	.917	.935	.944	.958	.988	-

Eigen Matrix Expressed as % of Contribution

1	2	3	Band
17.97	7.24	16.89	1
34.46	7.56	8.64	2
42.90	2.28	29.59	3
0.184	0.20	0.56	4
2.75	21.81	12.11	5
1.56	60.68	31.92	7

A 1024 x 1024 subscene that encompassed most of the features that we wished to delineate, including an ophiolitic complex, and available ground truth in the form of geologic mapping was chosen for detailed analysis of optimal color combinations for the base map. We recognized that compromise would be required for scenes of different dates and observed features. Table 4-2A shows the general interband statistics for this area. Table 4-2B presents the correlation matrix derived from the covariance matrix. A number of bands are highly correlated, but, overall, a lower degree of correlation exists than for the bands of 173,45 Q2 in Table 4-1. An eigen analysis for principal components (Table 4-2B) shows the relative contribution of each band to an eigen vector. Note that the first eigen vector has 93.9% of the total variance and that E_1 and E_2 have 97.6% of the total variance.

Table 4-2A: General Interband
Statistics, 1024 x 1024 Subscene of 172,45 Q2

Band 1	Band 2	Band 3	Band 4	Band 5	Band 7
Lower Triangle Cov. Matrix					
1					
366.927					
2					
256.023	201.866				
3					
422.919	315.881	534.732			
4					
322.294	246.550	410.804	338.441		
5					
610.834	457.089	768.869	619.643	1310.643	
6					
406.358	309.522	524.111	426.943	880.673	636.231
Mean Vector:					
113.492	56.298	78.524	61.076	122.698	80.236
Min. Vector:					
61.000	18.000	17.000	8.000	9.000	2.000
Max. Vector:					
205.000	129.000	200.000	166.999	255.000	183.000
Std. Dev:					
19.155	14.207	23.124	18.896	36.202	25.223
Eigen Values:					
.939	.037	.010	.006	.003	.003
Eigen Vectors:					
1					
-.316	-.237	-.396	-.316	-.631	-.432
2					
-.512	-.323	-.447	-.190	.461	.427
3					
-.398	.084	.205	.397	-.552	.573
4					
.579	-.134	-.123	-.504	-.282	.544
5					
.099	-.895	.384	.187	-.002	-.068
7					
-.363	.109	.661	-.644	.053	-.006
E_1	E_2	E_3	E_4	E_5	E_7

Table 4-2B: Correlation Matrix

for 1024 x 1024 Subscene, Derived from Covariance Matrix

Correlation Matrix

$$\text{Corr} = \frac{\text{Cov } [XY]}{\sigma_x \, \sigma_y}$$

	1	2	3	4	5	7
1	-					
2	94.08	-				
3	95.48	96.15	-			
4	91.46	94.36	96.57	-		
5	88.09	88.87	91.84	93.04	-	
7	84.11	86.38	89.86	92.01	96.45	-

Eigen Vectors = (eigen vector's)^2

Expressed as % of Contribution

	1	2	3	4	5	7
1	9.98	5.61	15.68	9.98	39.81	18.66
2	26.21	10.43	19.98	3.60	21.25	18.23
3	15.84	0.70	4.20	15.76	30.47	32.83
4	33.52	1.80	1.51	25.40	7.95	29.59
5	0.98	80.10	14.74	3.49	0	0.46
7	13.17	1.88	43.86	41.47	0.28	0

The statistical processing demonstrated that color combinations of bands 1,4,7 and 2,4,7 have lower correlation than other band combinations. Eigen vector bands were analyzed in the color-combination testing.

To corroborate the statistical band selections and to familiarize ourselves with the potential of certain color combinations to distinguish specific lithologies or structural features, we examined all possible combinations of the raw spectral bands in red, green, and blue (RGB). Each color combination was contrast stretched linearly for the best color image, and each received the same edge enhancement. Logarithmic and exponential contrast stretching at different histogram peak offsets were evaluated but not judged to be superior to the linear contrast stretch. Combinations were ranked with a letter grade. We sought the maximum color separation of image features regardless of the colors produced by a particular three-band combination. Hence, the same three bands in different combinations of RGB frequently received different grades (Table 4-3).

The top-ranking combinations were rerun. The final ranking is listed in Table 4-4. The top selection for the base map was 7,4,2 (RGB). This color combination with an edge enhancement was used to generate the base quad maps. Scaling for all quads was equivalent.

Eleven color-ratio combinations were evaluated; all were judged less superior to 7,4,2.

Color combinations of the eigen vector bands did not provide a useful selection for the base enhancement. However, these procedures were valuable for distinguishing finely detailed features and for distinguishing lithologies that appeared similar in 7,4,2.

Table 4-3: Graded RGB Band Combinations for Base Map

	1	2	3	4	5	7
1		123 D 124 D 125 D 127 D	132 B- 134 C 135 C- 137 B-	142 C- 143 C- 145 B 147 B	152 D 153 C- 154 B 157 B	172 C- 173 C- 174 C 175 C+
2	213 D 214 D 215 D 217 D		231 C 234 D 235 C- 237 D	241 C 243 C 245 C+ 247 C	251 C 253 C 254 B- 257 B	271 D 273 D 274 C- 275 B
3	312 C- 314 D 315 C+ 317 C	321 B- 324 E 325 D 327 D		341 D 342 E 345 C 347 C-	351 D 352 D 354 D 357 C+	371 C- 372 B- 374 C 375 B-
4	412 C- 413 C 415 B- 417 C+	421 B- 423 C- 425 C- 427 C-	431 B- 432 B+ 435 C- 437 C		451 C- 452 C- 453 C- 457 B-	471 C- 472 C- 473 C- 475 B-
5	512 C- 513 C- 514 B- 517 C-	521 B+ 523 B+ 524 B- 527 C-	531 A- 532 B- 534 C 537 C	541 A- 542 A- 543 B+ 547 C+		571 C- 572 C 573 C 574 B-
7	712 C 713 C- 714 C 715 C-	721 B- 723 C- 724 C 725 C-	731 A 732 B+ 734 C+ 735 C+	741 A 742 A+ 743 A- 745 B-	751 B 752 B+ 753 B 754 B+	

Table 4-4: Final Ranking of RGB Band Combinations for Base Map

Rank	R	G	B	
1	7	4	2	Final Selection
2	7	4	1	
3	7	3	1	
4	7	3	1	
5	5	3	1	
6	5	4	2	
7	7	3	2	
8	5	4	2	
9	5	2	1	
10	5	3	2	
11	7	5	2	
12	7	5	4	
13	7	4	3	

4.2 Digital Image Enhancement for Detailed Lithologic Discrimination

On a quad-by-quad basis, the following information was used to aid in developing the geologic interpretation:

1. published literature, including maps, whole-rock chemistry petrologic data, and age dates
2. signature extension
3. Full-resolution, CRT monitor mapping with optimized eigen vector band combinations (e.g.. Sheffield, 1985) and band combinations selected by digital-number responses of known lithologies in different lithologic assemblages.

With all of the basic geology in place on our 7,4,2 optimal base-map enhancement with constant, linear contrast stretching and edge enhancement, we dealt with details of structurally and lithologically difficult areas.

Following the algorithm of Sheffield (1985) to select the optimal TM- band subset from the variance/covariance information generated in Table 4-1 and 4-2, we obtained the rankings shown in Table 4-3. Top-ranked band combinations proved invaluable for discriminating lithologies in complicated geologic settings.

An additional technique was used to identify unknown lithologies using spectral signatures of known lithologies (digital modal or mean intensity vs band, hereafter referred to as "Digital Number" or "DN" technique). For instance, in 172, 45 Q4, digital numbers for ground-truthed lithologies within the Sol Hamed ophiolite complex and surrounding rocks were plotted on clear acetate overlays (Figure 3), and then DN signatures of unknown lithologies in previously unidentified ophiolites were compared to the known DN signatures. This procedure was carried out also for regions of Nafirdeib volcanics, Asoteriba (calc-alkaline) volcanics, sedimentary lithologies, sialic gneissic metamorphic zones, contact-metamorphic zones, and batholithic granite/younger granite bodies. Twenty-five regions of known lithology in scene 172, 45 and approximately eighty units of unknown lithology were identified by the DN technique. Graphs of key signatures are shown in Figure 3. These identifications helped to resolve problems in the geologic mapping and ultimately in the tectonic interpretation.

Table 4-5: Band-Combination Ranking
Based on Method of Sheffield (1985)

Rank	173,45 Q2	Determinant	1024 x 1024 Subscene of 173, 45 Q2	Determinant
1	531	16161722	753	4804541
2	541	9514956	751	4771848
3	731	8878091	531	3554187
4	751	8786194	541	3431861
5	741	5569835	754	2504626
6	521	5075912	752	2467124
7	753	4809682	521	2153708
8	721	2662933	731	2089930
9	752	2568368	543	2056927
10	754	2104181	741	1983089
11	532	1343434	532	1669968
12	542	1294364	721	1339116
13	543	1264883	542	1315990
14	742	760686	743	1181045
15	732	741200	732	1000257
16	743	740188	742	734766
17	431	707300	431	392621
18	432	399845	421	299418
19	421	285901	321	244318
20	321	60069	432	178448

4.3 Discrimination of Lithologies

Band combinations 5,3,1 and 7,3,1 in addition to 7,4,2 (RGB), with edge enhancement and linear contrast stretch examined at full resolution worked well for discriminating units within the ophiolites. This enhancement was used to resolve structure within the units as well. Figure 4 presents 8x10 inch reprints of Quads 1 through 4 of Scene 172,45 with acetate overlays of the interpreted geology.

4.3.1 Ophiolitic Rocks

Sol Hamed ophiolite units could be discriminated quite well in 7,4,2, in 7,3,1 and in 5,3,1. Figure 4 shows the digital-number response of Sol Hamed ophiolite units corrected for atmosphere scattering. In 7.3,1 the ultramafic units appear dark navy blue and are clearly discernible. The overlying gabbroic unit described as being in places a true serpentine melange "with disoriented gabbro blocks in a serpentinite matrix" (Fitches, et al., 1979). Melange development is clearly tectonic. Serpentinite matrix and brecciation noted the in field by other workers can be seen in the gabbro complex on TM imagery. Dark navy blue serpentinite mixed as fault slices and as matrix is distinguishable on the imagery.

4.3.2 Nafirdeib Volcanics

The volcanics generally appear reddish-orange on the 7,4,2 (RGB) false-color composite base maps, but dacite, gabbro and andesite mapped by El Nadi (1984) appear dark grey, similar to the metasediments. The topographic expression generally reflects structure. Apparent bedding on the scale of hundreds of meters usually is distinct and probably represents compositional variations, flow contacts, and variable amounts of intermixed sediments. Some units are more resistant to erosion and, thus, help define bedding. Wadis follow less resistant beds, joints, and faults. DN signature analysis accompanying characterization of topographic expression was used to discriminate and identify these lithologic units.

4.3.3 Nafirdeib Metasediments

A lens of conglomerate mapped in the field by Fitches, et al. (1983) northwest of the Oyo mine (east-central 172,45 Q1, Figure 4) appears dark bluish grey on the base composite. Fitches et al. also documented the location of pelitic rocks near the coast (southeast corner of 172,45 Q2) which appear dark grey on our base imagery. Flysch deposits mapped just northeast of the Sofaya ring complex in 172,45 Q4 are greyish brown and dark purplish grey. In the fold and thrust area of 172,45 Q4, El Nadi (1984) has field-mapped volcanics and "molasse" which are indistinguishable in 7,4,2. The unit appears similarly colored to verified occurrences of Nafirdeib volcanics in 7,4,2 band combination and has a similar DN signature across all bands.

The topographic expression of the metasediments is similar to that of the volcanics, facilitating interpretation of the structural geology.

4.3.4 Batholithic Granites

The batholithic granites are the pre- to syntectonic granites which intruded as part of a Pan-African island-arc. They cover extensive areas in the Red Sea Hills and are reported in field studies to form extensive areas of subdued sand-covered plains (El Nadi, 1984: Neary, 1976). Some batholithic granites also form areas of high, rugged relief. Both of these topographic expressions were encountered in this study, although the large batholithic intrusives tend to form sandy plains with inselbergs protruding through the alluvium (Almond, 1978; present study). Drainages form a medium-tight dendritic network and are shallow.

For intrusive units lacking radiometric dates, the prime discriminating factors were: the presence of deformational features indicating whether or not the intrusive appeared to have been involved in the collision event(s) that deformed the Nafirdeib Series rocks, and a spectral match to other batholithic granites.

The color of the batholithic granites on the 7,4,2 false-color composite photos varied from greyish tan to greyish brown to purplish brown. In the pluton that is faulted out by the northern limb of the Sol Hamed suture in the northwest corner of 172,45 Q1, probable hydrothermal alteration is evident in the area around the thrust fault ($22^{o}10$, $35^{o}30$, Figure 4). Similar color changes are seen in the southeast portion of quad 2 ($21^{o}43$, $36^{o}30$ is in the center of this area). Whether these color variations are a function of secondary hydrothermal alteration or variations in primary mineralogy of the pluton is not definable without field verification.

4.3.5 Young Granites

The Young Granites usually form high, rugged terrain 1000-1500 meters above the intruded area, but also form low, circular, sandy areas bounded by country rocks (El Nadi, 1984; Neary, et al. 1976 Greenberg, 1981). The resistant plutons have coarse polygonal drainage patterns that follow the geometry of joints and dikes, not dendritic patterns. The low, flat, circular plutons are sometimes sand covered, have dendritic drainage patterns, and, except for their structure, resemble batholithic granites.

The color on the 7,4,2 false-color photos is variable; it is pinkish grey to brownish grey to grey to brown. Many of the intrusives are circular and show multiple episodes of igneous activity, often with discernible compositional differences. Some young intrusives appear compositionally bimodal as gabbroic-granitoid. The gabbroic rocks are dark brown in the 7,4,2.

Young granites are post-tectonic and either crosscut previously existing structures or are intruded into preexisting zones of weakness.

4.3.6 Young Mafic Intrusives

Late mafic intrusive rocks, possibly related to the young granites, are found throughout northeastern Sudan (Vail, 1978; Almond, 1979; Kabesh, 1962).

They cross-cut all suturing structures and are generally circular in plan view. An excellent example is the apparently layered mafic intrusion that intrudes the edge of a gneiss dome (21^{o} 38', 35^{o} 10').

The color in 7,4,2 is dark grey to black, with a slight navy-blue component.

4.3.7 Nubian Sandstone

The Cretaceous (Vail, 1978; Whiteman, 1971) Nubian sandstone covers and crosscuts all other formations and, in the one large outcrop in the area, is noticeably higher in relief. Very few drainage channels are developed in the outcrop, but it is textured with long narrow linear features which are brown in color. The color on the 7,4,2 base maps is tan to light reddish brown.

4.3.8 Gneisses and Amphibolites

The gneissic terrains are low and hilly, in places covered with expanses of wind-blown sand (Kabesh, 1963). Drainage patterns are dendritic and form a dense, shallow network, often sand filled. Gneissic amphibolites are found in two places within this scene: as a gneiss dome in the west-central portion location, and as up-thrusted amphibolites and gneisses in the southeastern corner (Figure 4).

The color in 7,4,2 is light greyish brown in both areas. The spectral signatures across all seven bands differs from those of the Batholithic and Young Granites.

4.4 Recognizing Structural Features

El Nadi (1984) concluded, after his field work, that "the drainage system of the Red Sea Hills is generally structurally controlled, where most of the khors and wadis (wide khors) follow fault lines and structural joints, but their tributaries form dendritic patterns."

We mapped faults only where units were truncated or displaced in line with other truncations and displacements. We agree that faults are often marked topographically by saddles, wadis, and khors in the Red Sea Hills, as occurs in many other morphologically immature areas throughout the world. We mapped persistent, linear, topographically expressed features without distinguishable displacement or truncation as lineaments/joints. Some of these may be reclassified as faults with measurable displacement in the field, but displacement is not discernible using TM data. In some places, interaction of the fault plane with topography allowed an approximate dip determination. These dip estimates are plotted on the map. Prominent joint sets were mapped wherever present. However, all detectable joints are numerous and are not mapped to prevent obscuring of other significant data.

Folds were mapped in the Nafirdeib by mapping bedding strike-lines. Where the "law of v's" allows determination of dip on stratigraphic sequences, anticlines and synclines were discriminated. Dip symbols that were interpreted from imagery do not have numbers; dips taken from the literature do have numbers.

SECTION 5

5.0 RESULTS AND DISCUSSION

Three working map overlays were prepared for each quadrant. One map has the interpreted geology and was the main working overlay. The second has the literature "ground-truth" information plotted. These data include lithologies that were described in the field by previous researchers, petrologies, and geochronologies (Table 5-1) obtained from the literature. The third overlay is a lithotectonic map at a scale of 1:1,000,000 that emphasizes the continuity of regional trends within and beyond the study area. Figure 4 is false color 7,4,2 composite photos of Scene 172,45 (Quads 1 to 4) with overlays of interpreted geology.

5.1 Stratigraphy of Scene 172,45

5.1.1 Ophiolites

Tectonically disrupted ophiolite complexes are the oldest rocks in this scene. The Sol Hamed ophiolite ($22^{o}15'$, $36^{o}08'$), was named by Vail (1985), and has been studied in detail in the field by Fitches et al (1983). It has not previously been mapped. The Wadi Onib ophiolite ($21^{o}34'$, $35^{o}17'$) was briefly described by Hussein, et al. in (1982). On our base-map photos, we have discriminated the major lithotectonic units: ultramafic complex (Ou); gabbros and sheeted dike complex (Og); breccias with serpentinite matrix, pillow basalts, and overlying sediments (Ob). From the areas of known ophiolitic assemblages, we have extrapolated by spectral signature, topographic expression, and morphology to map their distribution along suture zones.

The ophiolitic complexes along the Sol Hamed suture appear to be soled by a thrust fault, and, spectrally and morphologically, appear to have a relatively consistent lithotectonic stratigraphy. Based on DN signature identification, the basal unit is ultramafic, variably serpentinized, with some interlayered gabbros (?). We have identified deformation in this unit

Table 5-1: Radiometric Dates in Scene 172,45

	Rock	Date	Method	Location	Reference
1.	Young Muscovite Granite	575 m.y.	Whole Rock K/Ar.	21°08'30N; 36°10'E	Technoexport (1974)
2.	Young Granodiorite	543± 18 m.y.	Rb/Sr	22°N.; 36°11' 30' E	Vail (1978)
3.	Young Alkali Granite	530± 2 m.y.	Whole Rock K/Ar.	21°14'N.; 36°15' E	Vail
4.	Granite Gneiss	580 m.y.	Whole Rock K/Ar.	21°00'N; 36N 15 'E	Technoexport (1974)
	Pegmatitic Granite	610 m.y.	Whole Rock K/Ar.	21°00'N; 36N 15' E	Technoexport (1974)
5.	Asoteriba Volcanics	649± 18 m.y.	Rb/Sr	(21°50'N.; 36° 32' 30" E)	Cavanagh (1970)
6.	Nafirdeib Volcanics	712± 54 m.y.	Rb/Sr	Between Sol Hamed and Wadi Onib (21°50'N.; 36° 32' 30" E)	Fitches, et al. (197_)
		543± 18 m.y.	Rb/Sr	22°N.;36° 11' 30"E	Vail (1978)
7.	Batholithic Granites	686± 18 m.y.	Rb/Sr	N.W. of Jebel Asoteriba (22°N.; 36° 25' E)	Cavanagh (1974)
8.	Batholithic Granodiorite, Small Stock	770 m.y.	Whole Rock K/Ar.	(21°15' 6"N.; 36° 20' 6" E)	Technoexport (1974)

to be isoclinal folding with some internal coherence. Overlying this is a gabbroic-volcanic and serpentinite melange that appears to be in fault contact with the basal unit. Flows and dikes are brecciated and cannot be followed over long distances. Serpentine forms a matrix to the breccia as stringers. Basaltic to andesitic volcanics overlie some of the interbedded sediments.

5.1.2 Nafirdeib Series

5.1.2.1 Volcanics

Unconformably overlying the Sol Hamed ophiolite are the Nafirdeib volcanics and associated sediments (Fitches et al., 1983). The volcanics have been identified by others as basalts and andesites with volcaniclastics and agglomerates. Petrologically and geochemically they are distinctly calc-alkaline and have close affinities to island-arc volcanism in other parts of the world (El Nadi, 1984). They are considered to be the early intra-oceanic island-arc volcanics, and have been dated at 712 m.y. (Fitches, et al. 1983) in the area covered by scene 172,45 Q2.

5.1.2.2 Metasediments

The associated Nafirdeib sediments have been described as flysch and molasse (El Nadi, 1984) and include conglomerates, greywackes, pelites, calcareous shales, sandstones, and minor limestone. These terms specifically imply a continental source for the clastics during convergence. However, there is no continental source for these clastics, only volcanic. Thus, we consider the sediments to be reworked volcanics derived from the Nafirdeib intra-oceanic island arc. The clastic rocks are composed of variably reworked volcanics identical in composition and in spectral signature to the Nafirdeib volcanics.

The volcanics that are interbedded with these metasediments are distinctly different from the Nafirdeib volcanics geochemically and petrologically. These are tholeiitic basalt flows with rare-earth chemistry that closely resembles marginal basin (analogous to a back-arc basin) volcanics (El Nadi, 1984). Back-arc basin volcanics are interfingered with island-arc volcanics, suggesting a back-arc or marginal-basin setting.

Nv is the symbol used for Nafirdeib volcanic rocks in the Nafirdeib series. Nc is the symbol used for clastic sediments. Nc-v represents intercalated volcanics and sediments. Na refers to Nafirdeib Series rocks that have been altered hydrothermally or metamorphosed by intrusive activity. The distribution of these rock types is shown on the map overlays of Figure 4 and on the 1:250,000 map, Plate 1.

Low-grade Nafirdeib series form moderate topography (El Nadi, 1984; Kabesh, 1962), except for the late Asoteriba volcanics, which constitute the highest, most rugged area.

The Nafirdeib volcanics and metasediments have been metamorphosed to greenschist facies field assemblages (El Nadi, 1984; Vail 1978) and are reported to have amphibolite facies assemblages in places.

5.1.3 Batholithic Granites

The batholithic granites are considered here to be pre- to syntectonic intrusives. Ages range in this scene from 770 m.y. to 545 m.y. Cavanagh (1979) dated batholithic granites (Rb/Sr) in the vicinity of Jebel Asoteriba (21^{o} 52', 36^{o} 30') at 686$\pm$ 18 m.y. The ages reported for these granites throughout the Arabian-Nubian shield vary from as old as 960 to 500 m.y. (Brown, 1980). Vail (1983) summaries geochronologic evidence as ranging from 900-650 m.y., with many in the 820-720 m.y. range.

Vail (1983) found no systematic spatial variation in lithologic ages in northeastern Africa. However, island-arc terranes of various ages have been distinguished in Saudi Arabia (Stoeser and Camp, 1985). The present study will lead to systematic age distributions of island-arc terranes in Sudan.

Rock types are heterogenous and include diorite, monzonite, granodiorite, and granites (Vail, 1983); tonalites predominate (El Nadi, 1984). Geochemically, the batholithic granites are calc-alkaline, typical of island arc granites (El Nadi, 1984) They show a systematic variation from west to east. From the Red Sea $K_2O/(K_2O+Na_2O)$ and total Rb increase westward for 90 km (El Nadi, 19 of 4). Granites in the western United States show an increase in these parameters eastward, where subduction was west to east. El Nadi interprets his findings to mean that the granites formed during westerly directed subduction within the studied arc. (see Plate Tectonic Model).

5.1.4 Young Granitic Series

The Young Granite series includes a range of compositional types and a large range of ages. Sillitoe (1979) considers them to have been emplaced during the Pan-African event 620-500 my. Vail (1978) discussed three episodes of intrusion of young granites: approximately 550 m.y., 230 my. and 50-100 my. No tectonic controls on these distribution are evident.

The young granites are named because they cross-cut deformation, so are essentially postorogenic. Cavanagh (1979) found that the older the granite, the lower the $^{87}Sc/^{86}Sr$ ratio, similar to batholithic granites. Thus, the evolution of more continental-type crust through time is seen in the Nubian shield.

Compositionally, the granites are typically alkaline although the oldest are calc-alkaline syenites, granites, and gabbros. Vein and disseminated mineralization is associated with less than 1% of the granites, generally in the late-stage, highly differentiated plutons (Sillitoe, 1979). Structurally they are found to be multi-stage, complex intrusives. They are generally circular or oval in plan, sometimes occurring as ring dikes. The Sofaya ring complex (21^{o} 18', 36^{o} 08') has been studied extensively. It has yielded seven K-Ar whole rock ages between 226 and 550 m.y., and two Rb/Sr dates of 394 ± 9 and 465 ± 9 (Vail, 1976).

5.2 Alteration and Metamorphism

5.2.1 Localized Contact Metamorphism

Alteration of the country rock surrounding plutons has been reported by Vail (1978) and Neary, et al. (1976). Obvious metamorphic and hydrothermal halos conform to the intrusive contact, discoloring contiguous rocks while only minimally disrupting their structure. TM spectral data proved excellent for mapping these features. In a study of granites in northeastern Sudan, Neary, et al. (1976) reported an area of assimilation in which a granitic batholith was extensively contaminated by the country rock. In the present study, the same region was independently identified as consisting of extensively metasomatized volcanics intruded by altered batholithic granites (172,45 Q2, north central portion). Other similar areas of hydrothermal alteration can be identified where unaltered rocks can be followed structurally into the altered zone. Many examples of this spectral expression are found.

The field designation of greenschist facies has generally been assigned to the volcanics and country rocks of the Nafirdeib Series. However, Vail (1978) reports amphibolite-facies metamorphism in the Precambrian shield rocks of this area. Kabesh and Afia (1959) report contact metamorphic assemblages in the Nafirdeib series rocks. Cordierite-biotite-quartz, andalusite-sillimanite-quartz, and wollastonite-diopside marbles are all high temperature, low-medium pressure assemblages. This is a point of concern for discriminating rock types, since the formation of new mineral phases in a rock changes its reflectance. The greater the extent of metasomatism (the exchange of chemical constituents between the rock and metamorphic fluid), the more likely it is that the spectral signature of the rocks has changed. We expect roof pendants to be highly altered and metamorphosed, and thus, to appear different spectrally.

Areas mapped by Gabert (1960) as Kashebib Series in 172,45 Q3 are considered here to be metamorphosed and metasomatized amphibolite facies Nafirdeib

Series rocks. They are roof pendants and xenoliths in batholithic granite; their metamorphic grade should be higher than elsewhere. One of these pendants includes metamorphic rocks in Jebel Kashebib, the type locality for the series in northeastern Sudan.

The significance of the high-grade Kashebib series metamorphic rocks is problematic, and previous investigators have defined it differently. Since the Kashebib type locality is interpreted as roof pendant metamorphism, it's significance as a separate unit is doubtful. We do not use the designation "Kashebib Series."

5.2.2 Regional Metamorphism

A belt of amphibolite-facies Nafirdeib metasediments and meta-volcanics (the paragneisses of El Nadi, 1984) are thrust-faulted against Nafirdeib metasediments at the eastern edge of 172,45 Q4. For this same area, (Gabert (1960) reports a northeasterly trending belt of amphibolite Nafirdeib group rocks. The mineral assemblage reported to occur in these metasediments is cordierite + garnet + kyanite + occasional sillimanite. This is not a contact metamorphic assemblage. Pressures greater than 4-6 kilobars (10-20 kilometers depth) and temperatures greater than 500 C are required (Turner, 1981). This represents a higher grade of metamorphism at distinctly deeper crustal levels than that affecting the Nafirdeib Series west of the thrust.

El Nadi (1984) describes the original lithology of the amphibolite gneisses as distinctly different from the Nafirdeib series, including quartzites which he describes as continental shelf-type deposits. But Kabesh (1962) reports quantities in the Nafirdeib Series in the Mohammed Qal area to the south; thus El Nadi may have simply been in an area of quantities. Whether the amphibolites are (Gabert) or are not (El Nadi) equivalent of the Nafirdeib series, the thrust is a significant suture.

5.3 Structural History

We have distinguished three generations of faulting and two generations of folding. NNE-trending folding and thrusting dominates the eastern portion of the scene. Primarily because El Nadi (1984) has mapped much of this area, the southern portion of Quad 4 was selected as an ideal area to compare ground-mapped structural geology with that discernible from the Landsat TM imagery. The general structural style is reminiscent of continental-margin fold and thrust belts that are observed world-wide. The first generation of folds and faults are the northeasterly fold and thrust belts. We consider dominant vergence to be to the northwest, corroborated by the occurrence in the far eastern portion of the scene of up-thrusted amphibolite-facies metasediments juxtaposed against greenschist-facies metasediments ($21^{o}15$, $36^{o}42$). Dip on the thrust is eastward, as determined from the image. Other presumed thrusts in the area dip both east and west. On most, the dip is not detectable.

The second episode of folding is northwesterly. The fold axes of the earlier folds are seen to be refolded into spectacular interference patterns (21^{o} 04'; 36^{o} 27').

The second episode of faulting that we distinguish is the set which we describe as northwesterly trending normal faults, possibly related to east-African graben faulting reported by others in Sudan (Salana, 1985) and central Africa (Bosworth, et al., 1986).

The third episode of faulting is ENE strike-slip faulting and jointing which post-dates the young granites and the Cretaceous Nubian sandstone. This episode likely is related to Red Sea rift transform faulting, as suggested by Ahmed (1982) for northeastern Sudan, and all the Red Sea rift cratonic borderlands by Garson and Krs (1976).

All structures are cut by the Red Sea Graben's bounding normal faults, and subparallel faults to the west.

The major suture along which the Sol Hamed and other ophiolites were emplaced is called here the Sol Hamed suture, after Vail (1985). It presently dips steeply to the northwest in places and more shallowly southeast towards its southern termination by a previously unidentified, younger, northerly trending shear zone. Everywhere, the ophiolites face up to the southeast and are faulted at their base. Ophiolitic rocks are thrust over the Nafirdeib volcanics and batholithic granites (?). The suture represents westerly transport of the upper plate relative to the lower plate.

The major north-trending fault zone, here called the Deraheib suture, terminates the Sol Hamed suture. The Deraheib suture appears to have a largely strike-slip displacement, and the width of the sheared and mylonitized rocks is considerable. The fault zone that accommodated most of the strain is 3 to 10 kilometers wide throughout the length, but en echelon and anastamozing parallel faults form a zone 20 km wide. The volcanics appear to be crushed up to 50 kilometers away. Primary bedding is obliterated; drainage is random and closely spaced; topography is uniformly low. Numerous late, north-trending sutures similar to this have been documented in the Arabian shield (Fleck, 1976), and maybe related. A second parallel suture also cuts the Sol Hamed suture through the left-center of the scene.

The age of these north-trending sutures is late to post-orogenic. They appear to be intruded by hundreds of dikes. No plutons cut them, except for a young granite located at the intersection of the Sol Hamed and younger transecting suture. The age of this young granite is not presently available.

5.4 Lithotectonic Belts

We identify five NNE-trending belts in scene 172,45 (Figure 5). The largest is a belt of batholithic granites 90-100 kilometers wide, approximately the same as the present exposure of the Sierra Nevada batholith in California.

This belt of batholithic granites is considered to be at or near the axis of a Nubian-aged island arc. It is flanked by two belts of Nafirdeib rocks intruded by small batholithic granites and young granites. To the southeast it is paralleled by a 30-50 kilometer wide fold and thrust belt composed of Nafirdeib bimodal volcanics and reworked volcanics. Calc-alkaline andesitic volcanics predominate; tholeiitic basalts are interbedded with the sedimentary rocks. In the southeastern corner, amphibolite facies Nafirdeib (?) rocks and Batholithic granites are thrust into tectonic contact with greenschist-facies Nafirdeib series. The relationships among these rock types are discussed in Section 5.5, Plate Tectonic Model.

The batholith is flanked to the northwest by the Sol Hamed suture and its associated ophiolites, representing abducted oceanic crust. Unconformably overlying the ophiolite, Nafirdeib volcanics are also found to the northwest of the batholith. The Sol Hamed suture juxtaposes the batholith with rocks that have very few or no batholithic intrusives; this suture is younger than the island arc roots represented by the batholith.

The dominant vergence direction inferred by the Sol Hamed suture and the geometry of other thrust faults is northwesterly.

5.5 Plate Tectonic Model

5.5.1 Current Tectonic Models

Current tectonic models hold that the Nubian Shield of the Red Sea Hills of Sudan, together with the Arabian Shield of southwestern Saudi Arabia, are the northward extension of the African Proterozoic continental margin, represented by the Mozambique Mobile Zone of Holmes (1951). Burke and Dewey (1972) suggest that the mobile zone in southern and eastern Africa is a broad zone of deposition and deformation representing the collision and suturing of two continents. Farther north in Sudan, Egypt and Saudi Arabia, however, the character of rocks in the mobile zone changes; island-arc type intermediate volcanic rocks predominate, ophiolite belts are present, and sialic continental basement appears to be absent (Greenwood et al., 1980; Gass, 1979; Schmidt et al., 1979). The Nubian-Arabian Shield complex thus appears to represent the accretion of island-arcs, intervening oceanic

depositional basins, and trapped oceanic crust onto the older African craton to the west (present study, Greenwood et al., 1980). An alternative hypothesis proposed by Garson and Shalaby (1976) and Delfour (1981) suggests that rifting of an earlier cratonic margin may have occurred in this area along the mobile zone, and that subsequent accretion along the zone included the collision of rendered microcontinents as well as trapped oceanic crust and island-arc complexes.

Tectonic studies in Saudi Arabia indicate that island-arc accretion occurred from west to east (Stoeser and Camp, 1985), and that the sutures between accreted terranes should cross the Red Sea into eastern Sudan and Egypt (Vail, 1985, 1983; Stoeser and Camp, 1985; Camp, 1984; Shackleton, 1986). The direction of plate convergence and number of accretionary and orogenic events is not well known. Lateral translocation and accretion of exotic terranes has not been evaluated.

Many recent workers favor the idea that several island arcs, even as many as ten (Gass, 1982), accreted to the Arabian-Nubian shield during the Proterozoic (Almond, 1978; Gass, 1977; Shackleton, 1979, 1986; Stoeser and Camp, 1985). These concepts were developed first on the Arabian side of the shield where mapping is more complete and radiometric dating provides a clearer picture of the geochronology. Recognizing individual island arc packets is complicated on both sides by the fact that several arcs with differing polarity and ages have been superimposed.

5.5.2 Tectonic Model Derived From TM Study

We see abundant evidence for collisional accretion of island arc terranes in the northern Red Sea Hills. But we also see major N-S strike slip sutures (i.e., the Deraheib suture) with ultramafic rocks along them that displace accretionary boundaries. We do not believe that every belt of ophiolitic rocks represents a subduction zone. Some ophiolites may have been obducted by the mechanism of back-arc thrusting, which is considered to be

the mechanism for obduction of the Troodos ophiolite in Cyprus, among others. This mechanism may have been active along the long-lived, Nile craton plate margin. El Nadi (1984) noted that the Nafirdeib sediments contain interbedded tholeiitic basalt flows, which are geochemically typical of marginal-basin basalts. We are developing an island-arc model which includes recognition of the back-arc basin rocks and their structural setting.

The Nafirdeib volcanics (712 m.y.) and batholithic granites (648-770 m.y.) in this batholithic belt are very similar geochemically, virtually indistinguishable geochronologically, and considered to be approximately contemporaneous (Neary, 1976, present study). The batholith-volcanic complex probably represents an island arc that developed from early extrusives and associated sediments, to later batholithic plutons intruding a deforming volcano-sedimentary prism. The axis that is exposed is mid- to upper level of the later arc. Higher levels are exposed to the northeast, where extensive contamination and roof pendants are abundant, and the late, but pene-contemporaneous Asoteriba volcanics overlie the batholithic granite (present study; Neary, 1976; Cavanagh, 1979).

The lithotectonic belts southeast of the arc axis are a Nafirdeib volcanic pile, essentially barren of intrusives, and tectonically juxtaposed against the batholithic arc. Marginal basin sediments and volcanics are faulted against these to the southeast. Amphibolites of significantly higher metamorphic grade (and possibly another arc?) are thrust westward over this belt.

Figure 6a shows a typical Phanerozoic island arc configuration modified from Almond (1978), who compared this model directly to the less-known island arcs in the Nubian shield. This model fits the packet of five belts in scene 172,45 (Figure 5) well. The Sol Hamed suture represents the paleo-subduction zone; the batholithic island arc intruding volcanics is the next lithotectonic unit; the back arc basin sediments and volcanics are next. Figure 6b shows a sequence of obduction of the arc along a suture (which would contain ophiolites). In this scenario, the fold and thrust

belt is developed in the back-arc basin during collision; imbricate thrusts and folding deform the ophiolite volcanic-sedimentary pile. Note that dominant vergence of all structures in the collision zone is to the west, and subduction is to the southeast, in agreement with Shackleton (1986), and the stress regime inferred by Camp (1984) for the same suture in Saudi Arabia (Figure 7).

The equivalent of the Sol Hamed suture extends across the Red Sea into the Arabian portion of the Nubian-Arabian shield (Figure 7). It is called the Bir Umq suture by Stoeser and Camp (1985), the Halaib Yanbu discontinuity by Camp (1984), and the Al Wask ophiolite complex by Vail (1983). Because of the similarity of Stoeser and Camp's interpretation to ours, we call this extension the Bir Umq suture.

Stoeser and Camp believe that the Bir Umq suture separates two island arc terranes, the Hijaz terrane to the northwest that is 700-800 m.y. and the Asir terrane to the southeast. The Asir terrane is also 700-800 m.y. in age over a region extending 200 km south of the suture, beyond which it is 800-900 m.y. (Figure 7).

This suture is morphologically similar to the Sol Hamed suture in Sudan. Ophiolitic assemblages are thrust together with greenschist-facies, arc-related volcanics and sediments. Isoclinal folds are common, as are imbricate thrust faults. Stoeser and Camp conclude that the Bir Umq suture appears to be the former site of a south-dipping subduction zone that ceased when the terranes collided sometime after 715 m.y. The Bir Umq suture is truncated by the north trending Nabitah suture that also contains ophiolite assemblages, and is a major crustal mobilization with westward-directed nappes. The Nabitah suture formed between 640 and 680 m.y.

SECTION 6

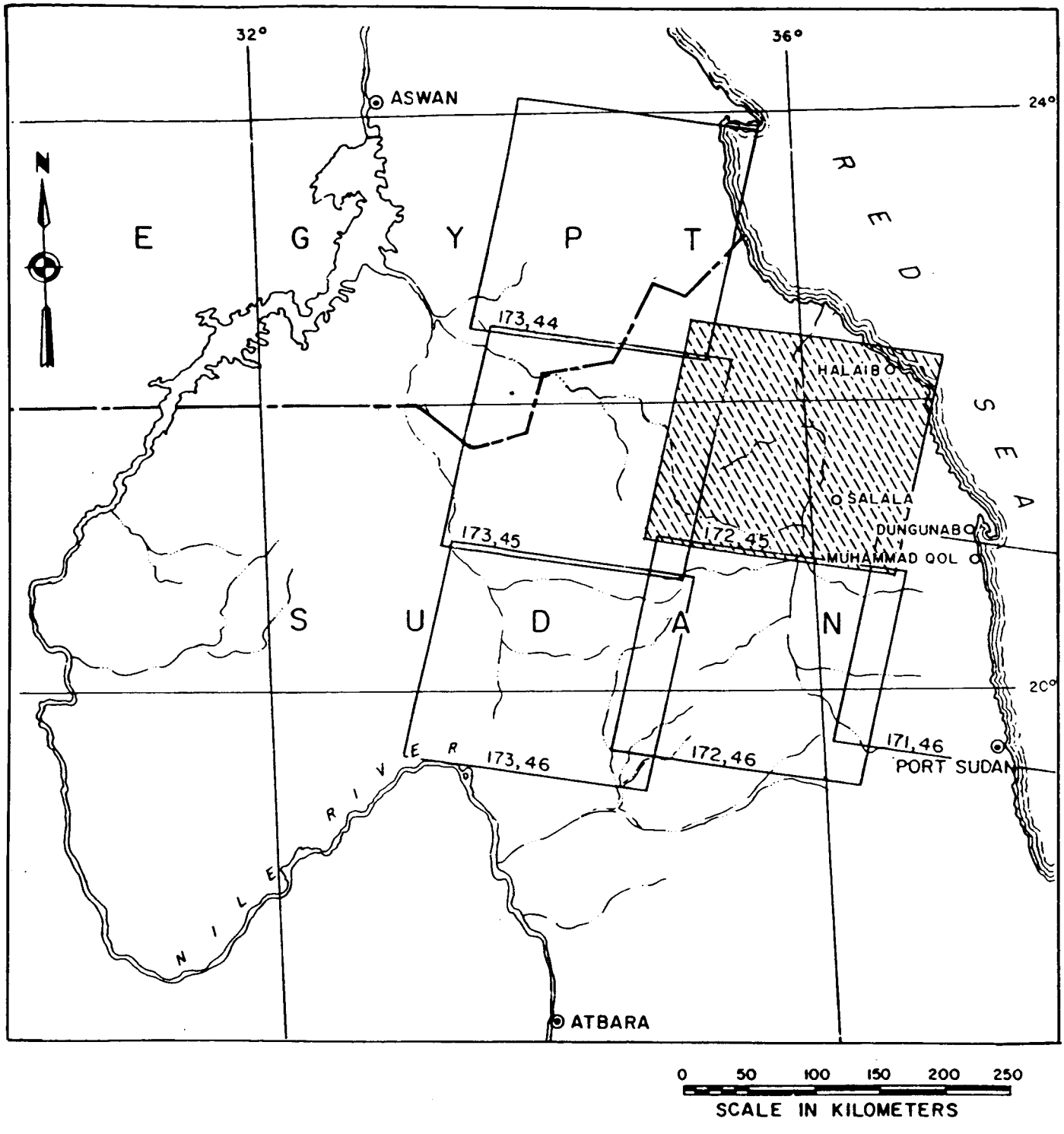

Figure 1. Location map of LANDSAT TM scenes.

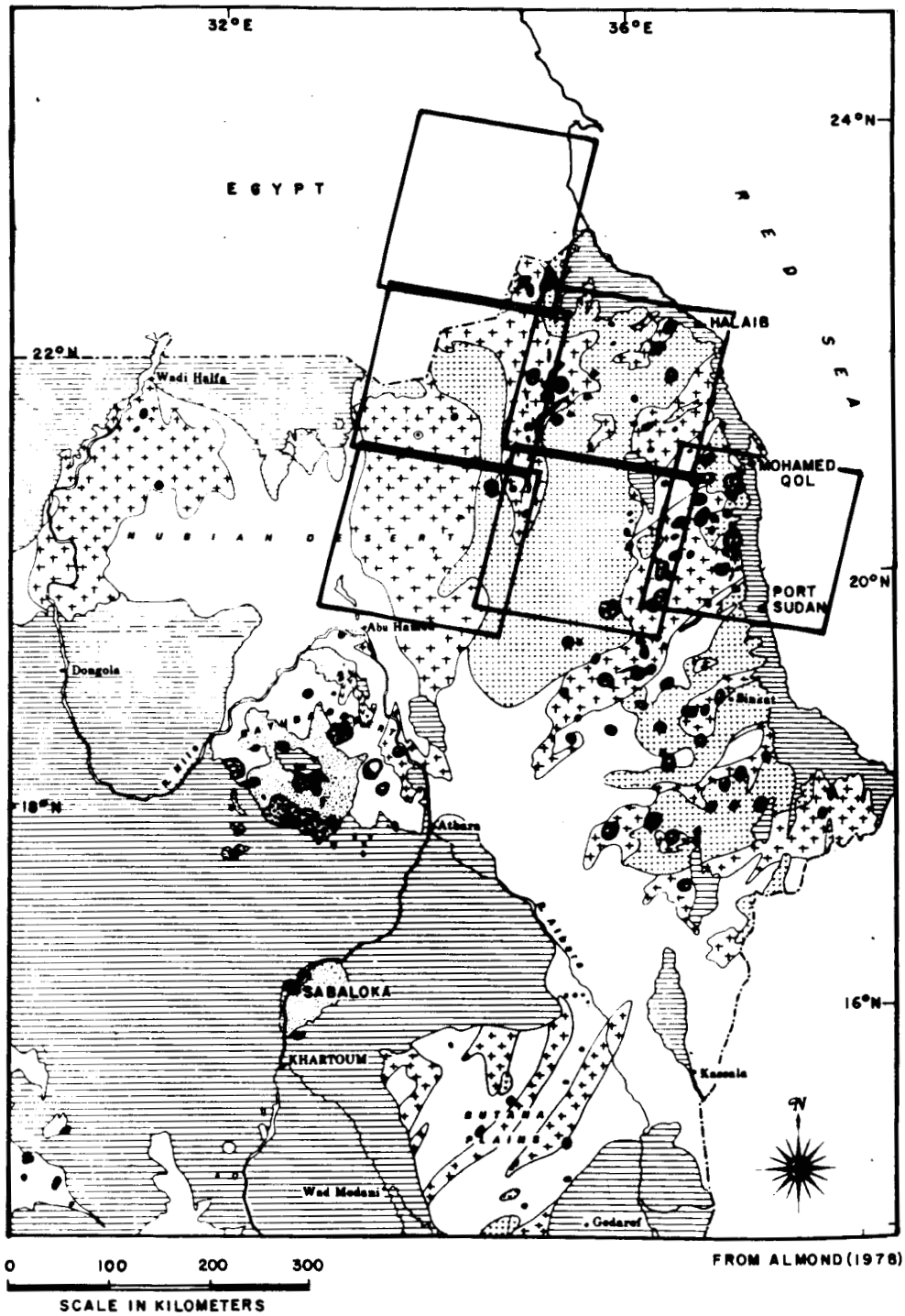

Figure 2. Generalized geologic map of northeastern Sudan. Plusses are low grade metamorphic rocks, horizontal rule is cover series, small v's are batholithic granites, dots are high grade metamorphic rocks, circular features are young ring complexes, black units are ophiolites.

FIGURE 3: DIGITAL NUMBER PLOTS (NOT CORRECTED FOR ATMOSPHERIC SCATTERING)
BATHOLITHIC GRANITES, 172,45 Q2

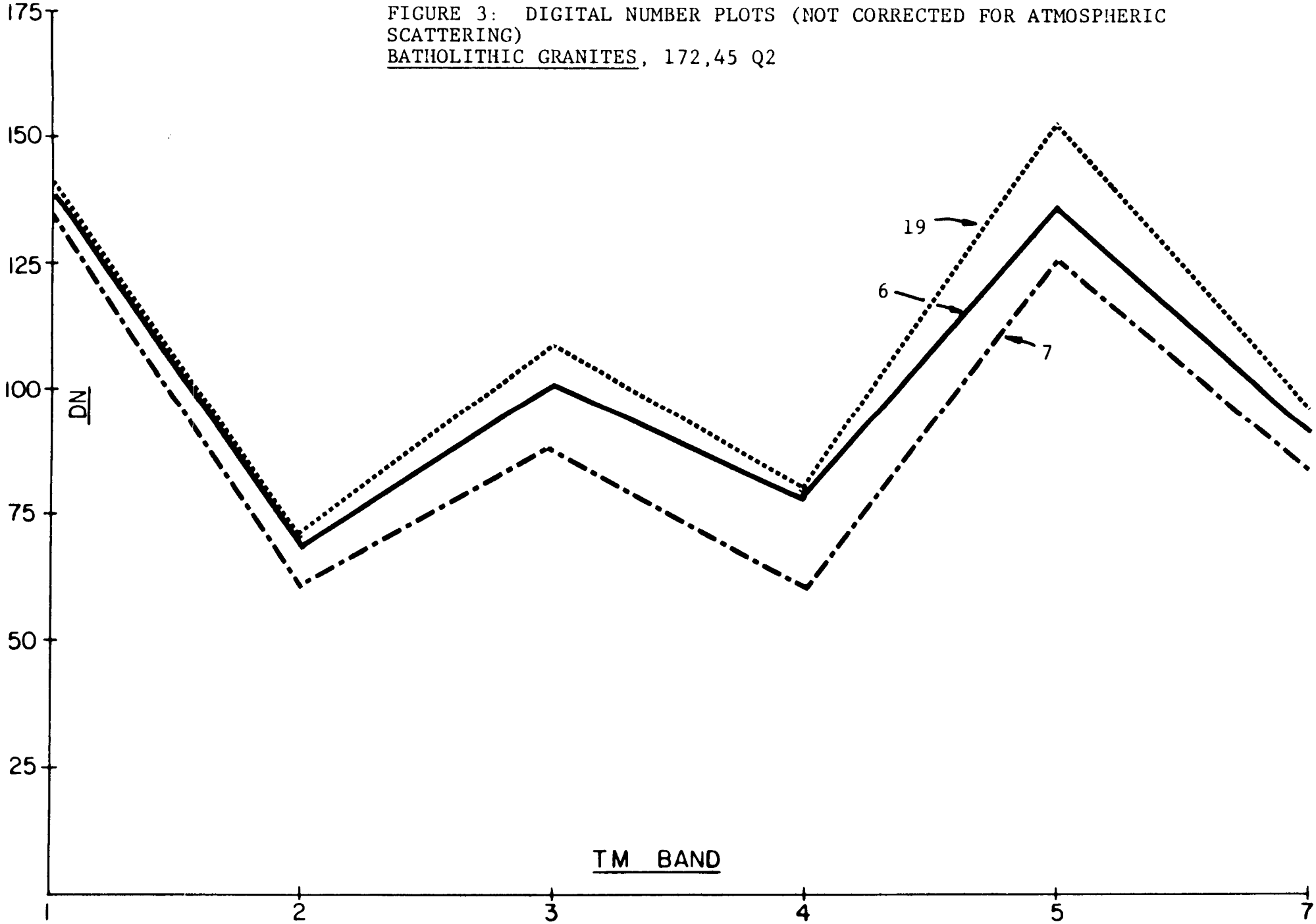

FIGURE 3: DIGITAL NUMBER PLOTS (NOT CORRECTED FOR ATMOSPHERIC SCATTERING)
YOUNG GRANITES, 172,45 Q2.

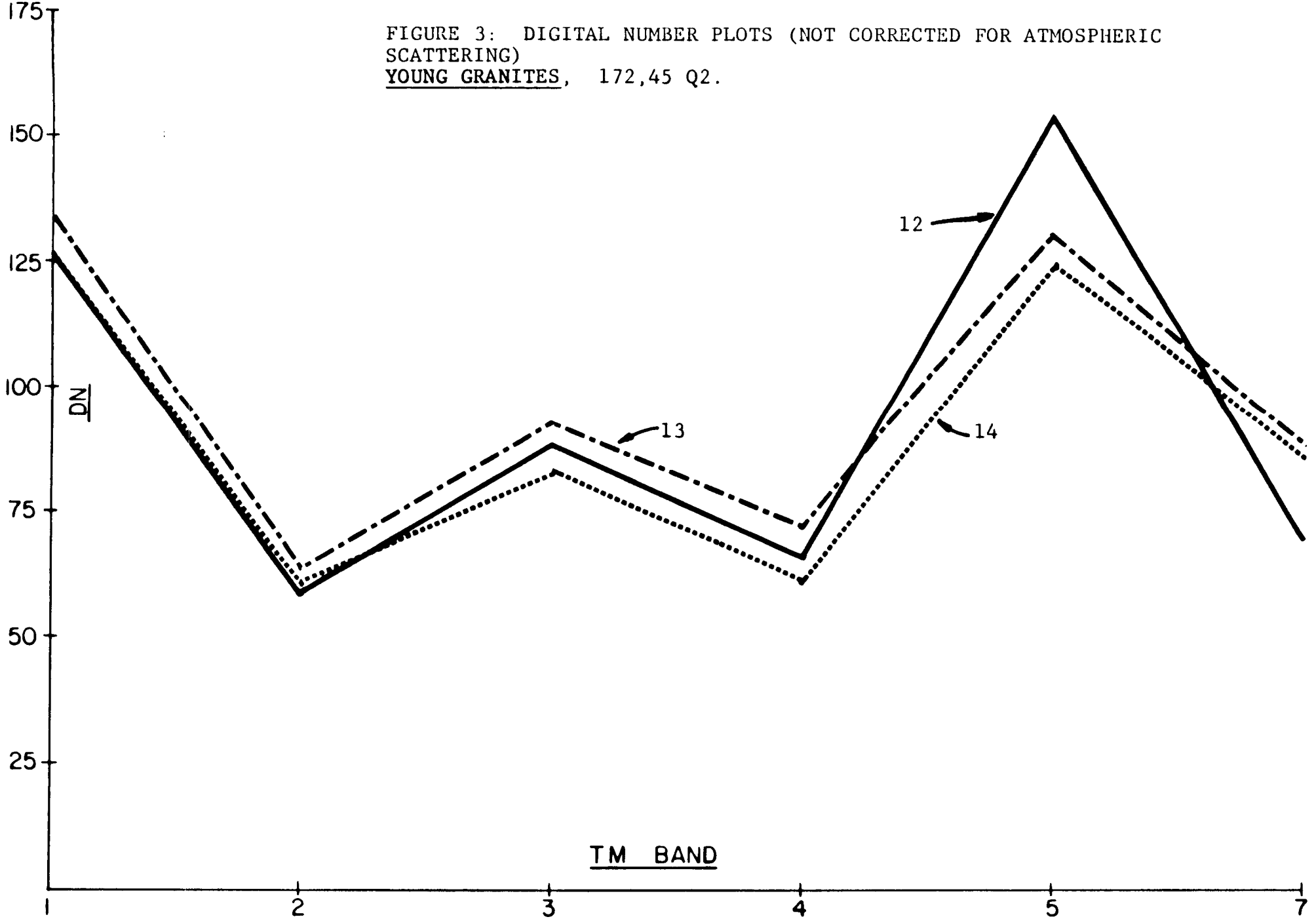

FIGURE 3: DIGITAL NUMBER PLOTS (NOT CORRECTED FOR ATMOSPHERIC SCATTERING)
VOLCANICS, 172,45 Q2

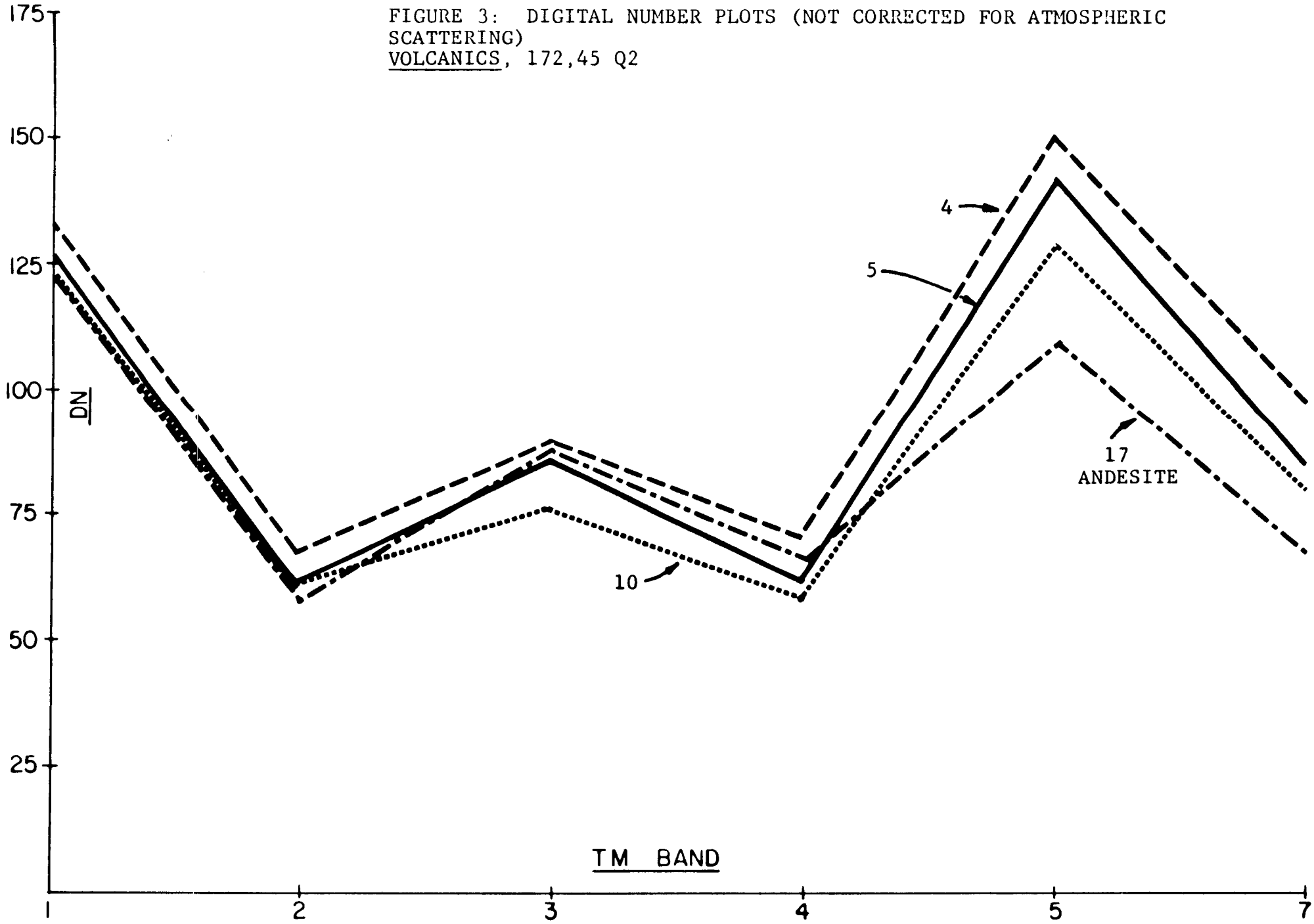

FIGURE 3: DIGITAL NUMBER PLOTS (NOT CORRECTED FOR ATMOSPHERIC SCATTERING)
ULTRAMAFICS, 172,45

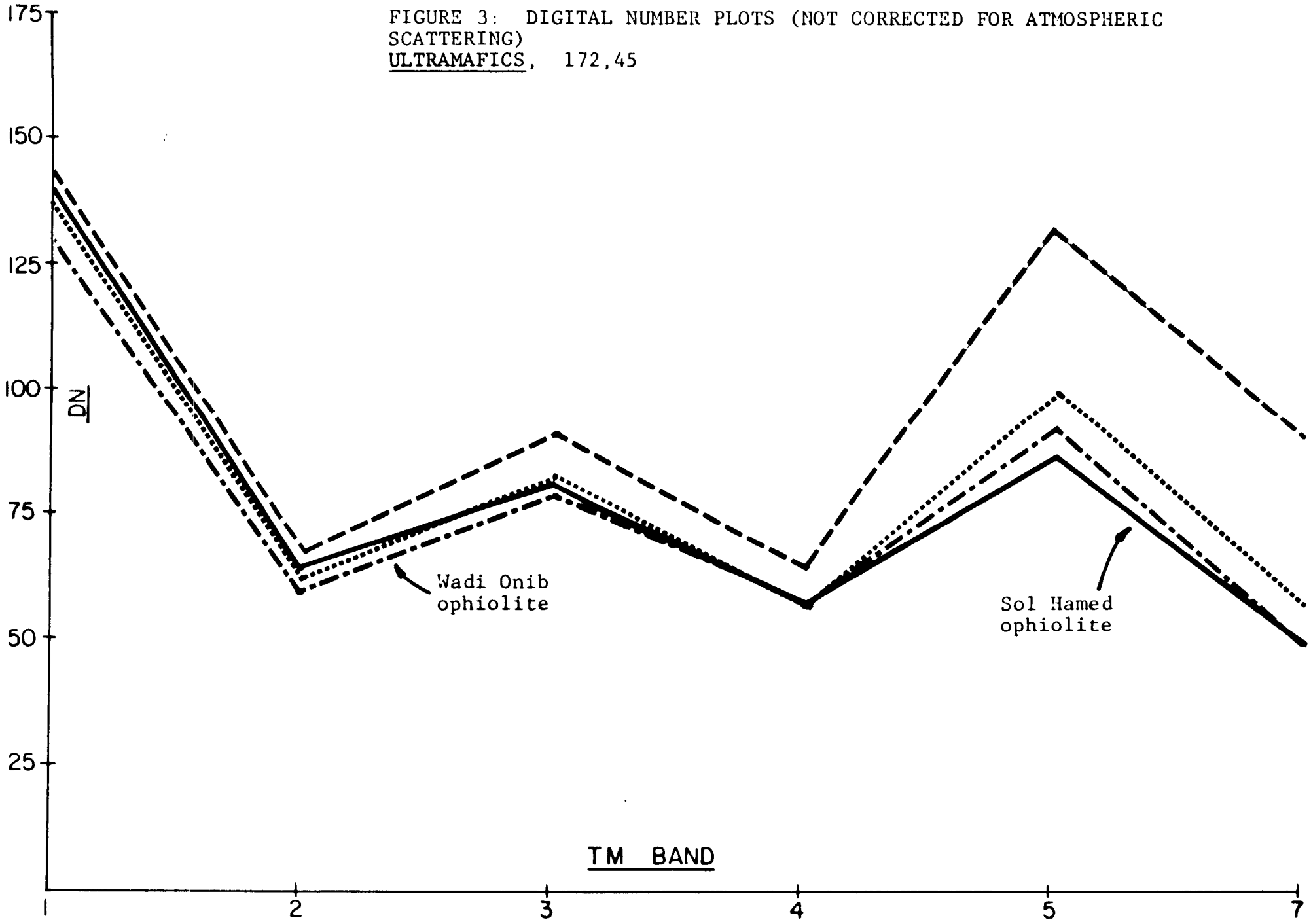

FIGURE 3: DIGITAL NUMBER PLOTS (NOT CORRECTED FOR ATMOSPHERIC SCATTERING)
SEDIMENTARY ROCKS, 172,45 Q2.

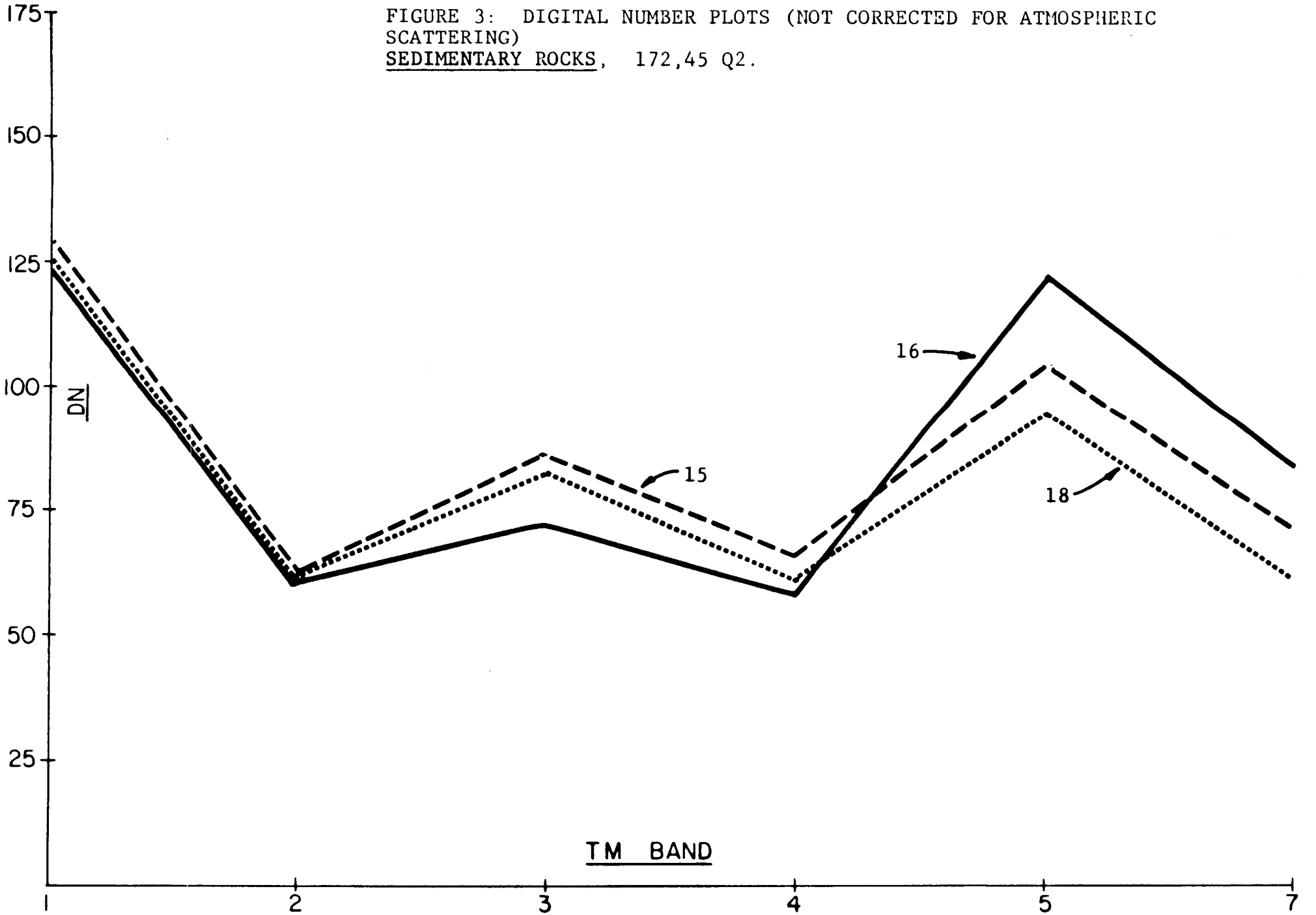

FIGURE 3: DIGITAL NUMBER PLOTS (NOT CORRECTED FOR ATMOSPHERIC SCATTERING), UNKNOWN LITHOLOGIES. 172,45 Q3.

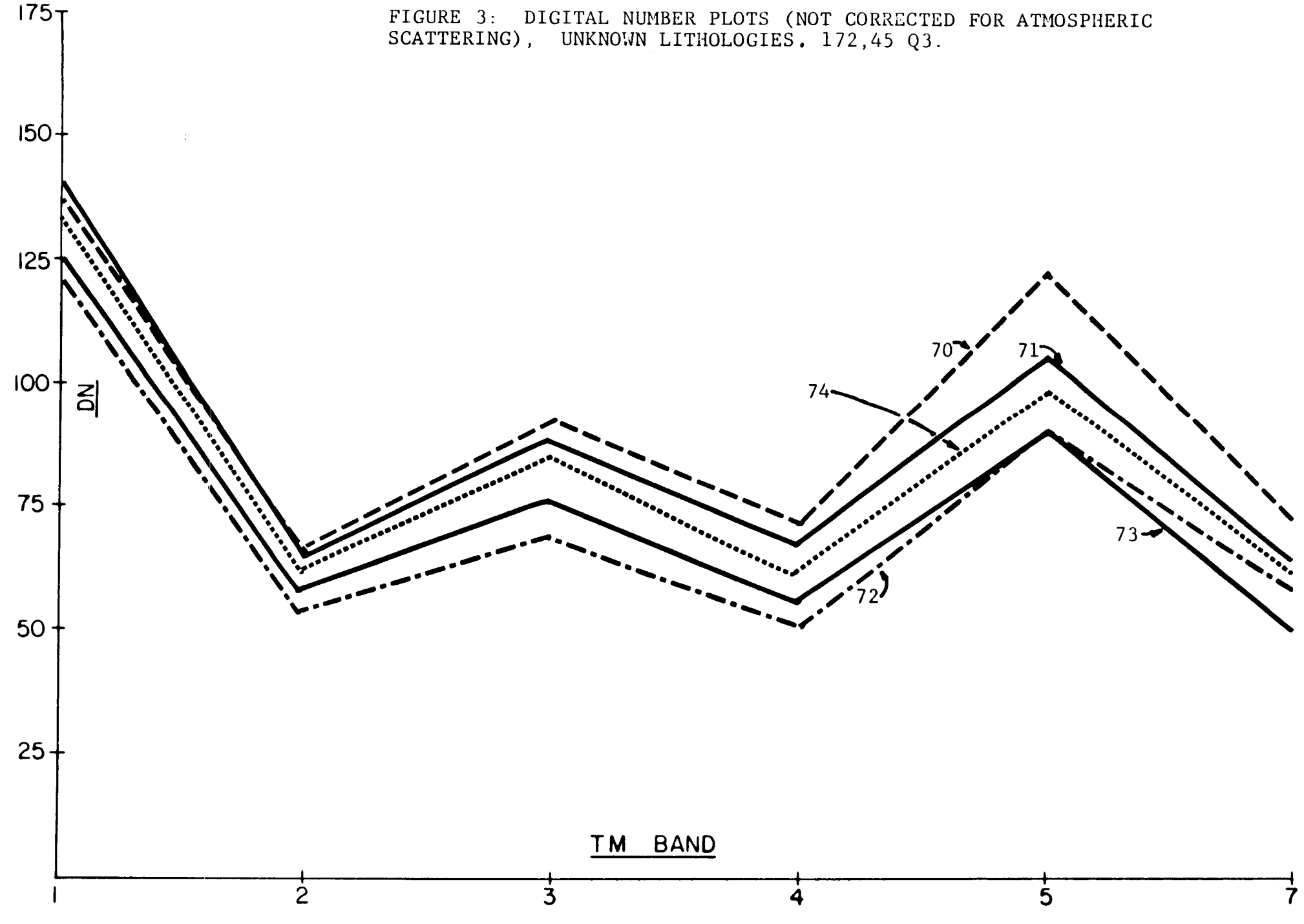

FIGURE 3: DIGITAL NUMBER PLOTS (NOT CORRECTED FOR ATMOSPHERIC SCATTERING), UNKNOWN LITHOLOGIES, 172,45 Q3

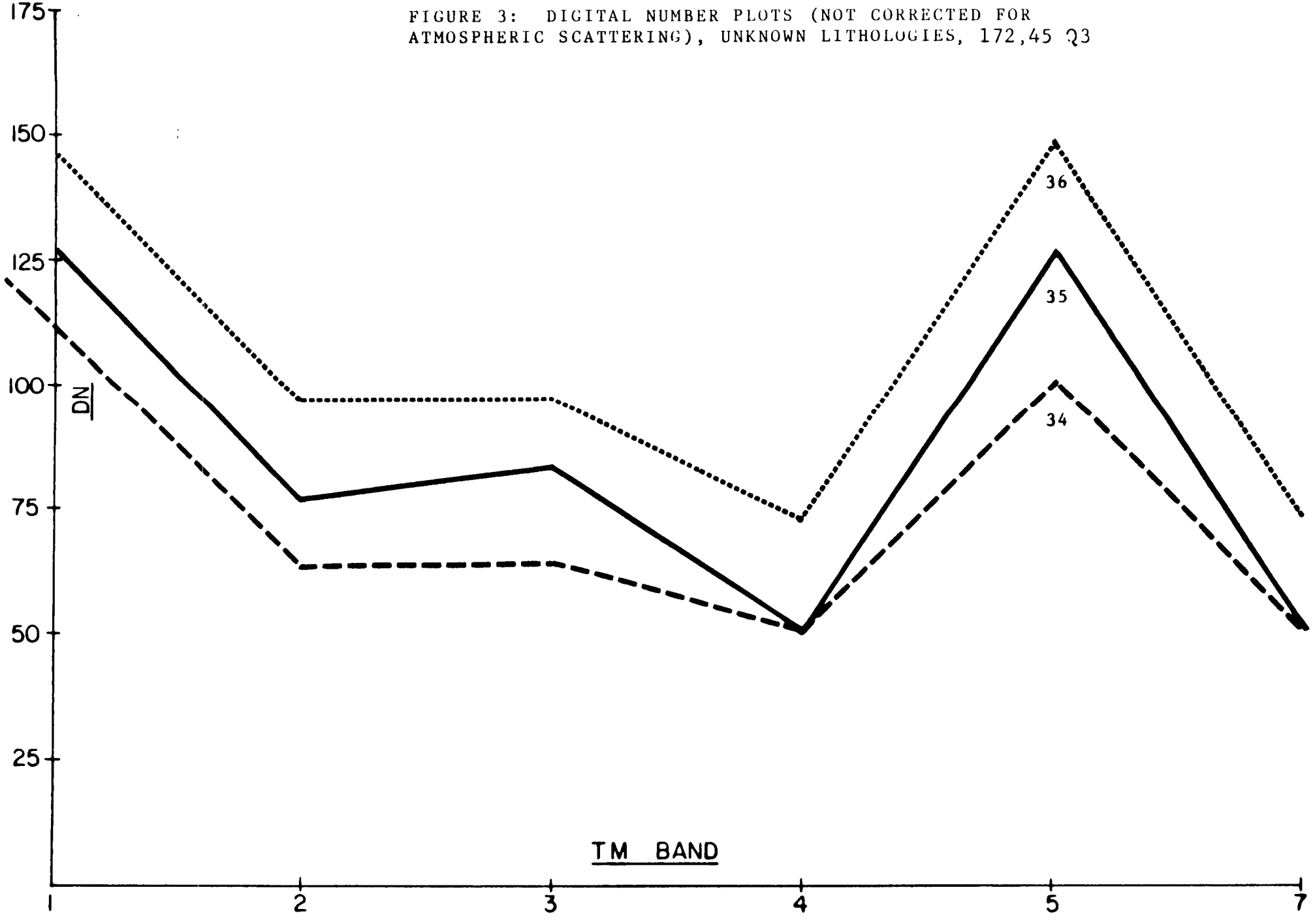

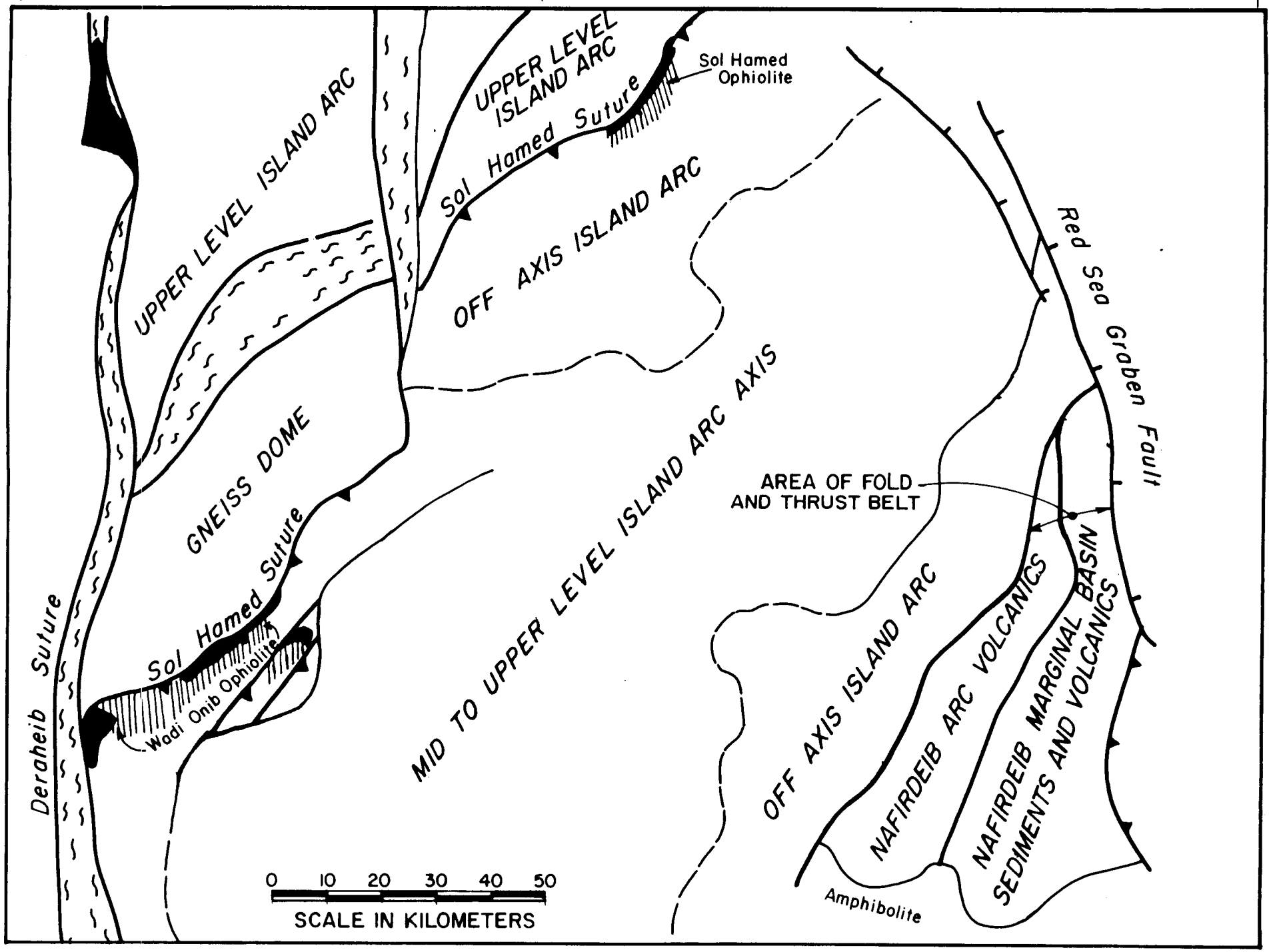

Figure 5. Lithotectonic belts in scene LANDSAT TM scene 172,45.

FIGURE 4: 172,45 QUAD I

FIGURE 4: 172,45 QUAD 2

FIGURE 4: 172,45 QUAD 3

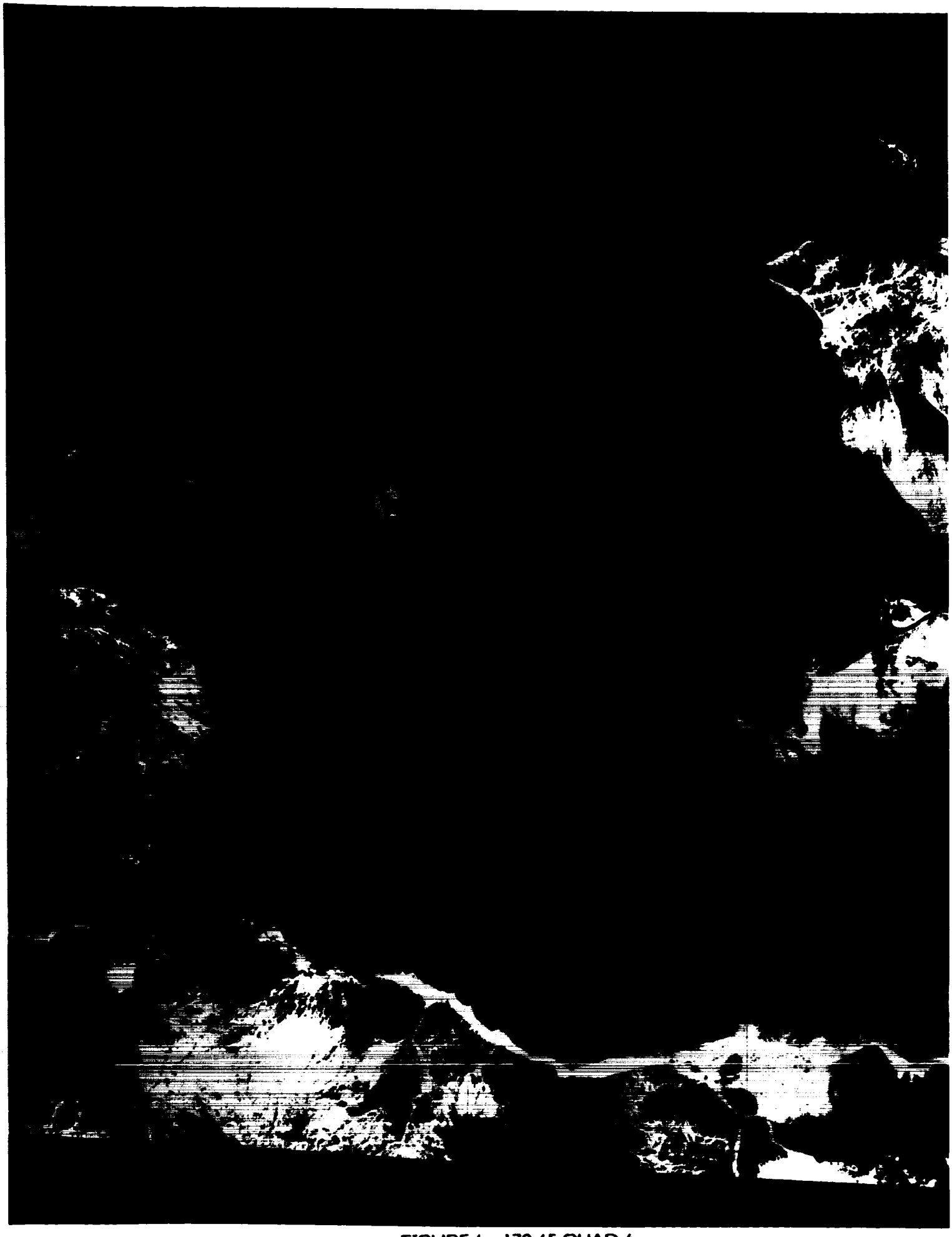

FIGURE 4: 172,45 QUAD 4

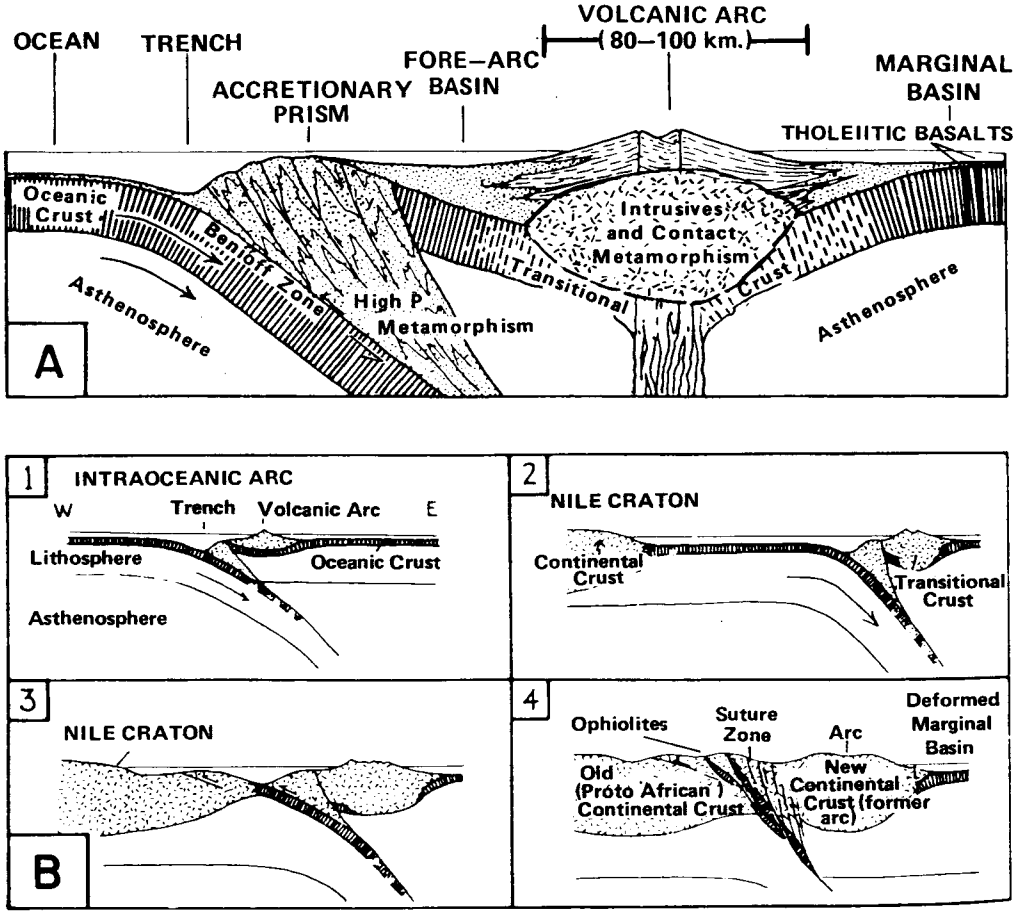

(after Almond, 1978)

A. Schematic section across a typical Phanerozoic island arc, showing the main Lithotectonic units. This distribution fits that seen in the Sol Hamed Suture area of the Red Sea Hills. The Red Sea Hills represents multiple island arcs and collisions along the Proterozoic Nubian Shield Margin.

B. (1, 2) Development of an intra-oceanic island arc (3, 4) collision and emplacement of Ophiolites intermixed with arc volcanics and sediments. If subduction now began from left to right, the Nafirdeib arc would be overprinted by deformation and plutonism from the newer arc.

Figure 6. Plate tectonic models.

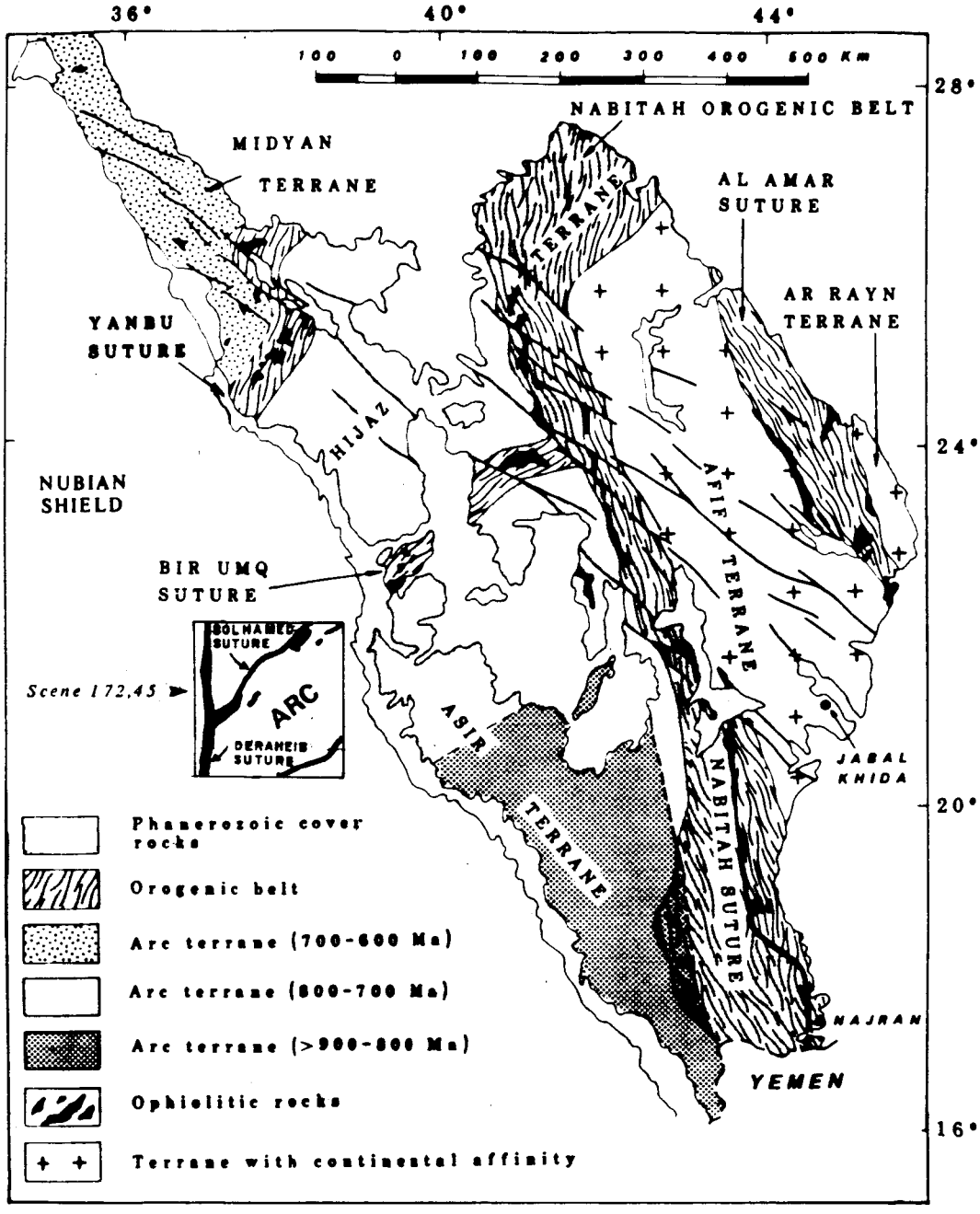

Figure 7. Palinspastically restored position of LANDSAT scene 172,45 (after Vail (1985) with respect to Arabian Shield terranes. Arabian terrane map from Stoesen and Camp (1985).

SECTION 7

A

Abdel-Khalek, M.L., 1979. Tectonic Evolution of the Basement Rocks in the Southern and Central Eastern Desert of Egypt, Inst. of Appl. Geology Bull. No. 3, King Abdul Aziz Univ., Jeddah, Kingdom of Saudi Arabia, Evolution and Mineralization of the Arabian Nubian Shield, p. 53-62.

Ahmed, A.A.M., 1979. General Outline of the Geology and Mineral Occurrences of the Red Sea Hills, Democratic Republic of Sudan, Ministry of Energy and Mining, Geological and Mineral Resources Department, Bull. No. 30, 69 p.

Ahmed, F., 1982. Implications of the Precambrian Lineaments on the Red Sea Tectonics Based on Landsat Study of Northeast Sudan, Global Tectonics and Metallogeny, Vol. 1, No. 4, p. 326-335.

Ahmed,, F., 1983. Sudan's Mineral Deposits, Mining Magazine, Vol. 148, No. 1, p. 31-35.

Almond, D. C., 1978. New Ideas on the Geological History of the Basement Complex of North-East Sudan, Sudan Notes and Records, Vol. LIX, p. 106.

Almond, D.C., 1982. The Concepts of 'Pan-African Episode Mozambique Belt' in Relation to the Geology of East and Northeast Africa, Precambrian Res., Vol. 16, No. 4, p. A4.

Almond, D.C., 1979. Younger Granite Complexes of Sudan, in Al-Shanti, A.M.S. (ed.), Evolution and Mineralisation of the Arabian-Nubian Shield, Vol. 1, King Abdul Aziz Univ., Inst. Appl. Geol. Bull. 3, Pergamon Press, Oxford-New York, p. 151-164.

Almond, D.C., Ahmed, F., and Dawoud, A.S., 1982. Tectonic, Metamorphic and Magmatic Styles in the Northern Red Sea Hills of Sudan, Precambrian Res., Vol. 16, No. 4, p. A4-A5.

Al-Shanti, A.M.S., and Roobol, M.J., 1979. Some thoughts on Metallogenesis and Evolution of the Arabian - Nubian Shield Inst. of Applied Geology (I.A.G. Bulletin #3) King Abdul Aziz Univ., Jeddah, Kingdom of Saudi Arabia, Evolution and Mineralisation of the Arabian-Nubian Shield, p. 87-96.

Anon., 1972. Guide to Mineral Investment in the Sudan, Rep. Geol. Survey Sudan, 44 p., Unpublished

Arnold, Guy, 1984. Sudan: Middle East Review, p. 255-259.

A

Aye, F., Cheze, Y., and El Hindi, M.A., 1985. Discovery of a Major Massive Sulphide Province in Northeastern Sudan, in Prospecting in Areas of Desert Terrain, London, The Institution of Mining and Metallurgy, p. 43-48.

B

Balkhanov, V.V., and Razvalyayev, A.V., 1979. The Origin of the Manganese Deposits of the Western Shore of the Red Sea. (In Association With Rifting), Internat. Geology Rev., Vol. 23, No. 2, p. 162-166.

Barr, D., Holdsworth, R. E., and Roberts, A. M., 1986. Caledonian Ductile Thrusting in a Precambrian Metamorphic Complex: The Moine of Northwestern Scotland, Geological Society of America Bulletin, Vol. 97, No. 6, p. 754-764.

Bechtel, 1983A. Applications of Remote Sensing Techniques to Mineral Exploration in the Republic of the Sudan, 48 p, unpublished report.

Bechtel, 1983B. A Comparative Study Between Minealization in Western Saudi Arabia and Northeastern Sudan, 45 p, unpublished report.

Bentor, Y. K., 1985, The Coastal Evolution of the Arabo-Nubian Massif with Special Reference to the Sinai Peninsula, Precambrian Research, Vol. 28, p. 1-74.

Blodget, H. W., 1977. Lithology Mapping of Crystalline Shield Test Sites in Western Saudi Arabia Using Computer-Manipulated Multispectral Satellite Data: Unpublished Ph.D. Thesis, George Washington University.

Blodget, H. W., Andre, C.G., and Marcell, R. F., 1985. Enhanced Rock Discrimination Using Landsat-5 Thematic Mapper (TM) Data, 1985 ACSM-ASPRS Fall Convention Technical Paper, Indianapolis.

Blodget, H. W. and Brown, G. F., 1982. Geological Mapping by Use of Computer-enhanced Imagery in Western Saudi Arabia: U.S. Geologic Survey Professional Paper 1153, 10 p.

Blodget, H. W., Gunther, F. J., and Podwysocki, M. H., 1978. Discrimination of Rock Classes and Alteration Products in Southwestern Saudi Arabia with Computer-Enhanced Landsat Data, NASA Technical Paper 1327, 34 p.

B

Brown, G. C., 1980. Calc-alkaline Magma Genesis: The Pan-African Contribution to Crustal Growth, in Al Shanti, A.M.S. (ed.), Evolution and Mineralisation of the Arabian-Nubian Shield, I.A.G. Bulletin 3, 3, p. 19-29.

Brown, G. F., and Jackson, R.O. 1979. An Overview of the Geology of Western Arabia, Instit. of Appl. Geology. Bull. No. 3, King Abdul Aziz Univ. Jeddah, Kingdom of Saudi Arabia, Evolution and Mineralization of the Arabian-Nubian Shield p. 3-10.

Brown, G.F., and Jackson, R.O., 1979. Geologic Map of the Asir Quadrangle, Kingdom of Saudi Arabia, U.S. Geological Survey Map I-217A, Scale 1:500,000.

Brown, G. F., Jackson, R.O., Bogue, R. G., and Elbert, E. L. Jr., 1963. Geologic Map of the Northwestern Hijaz Quadrangle, Kingdom of Saudi Arabia, U.S. Geological Survey Miscellaneous Geologic Investigations Map I-204A, Scale 1:500,000.

Brown, G. F., 1970. Eastern Margin of the Red Sea and the Coastal Structures in Saudi Arabia, Royal Society of London Philosophical Transactions, A, Vol. 267, p. 75-87.

C

Camp, V. E., 1984. Island Arcs and Their Role in the Evolution of the Western Arabian Shield, Geol. Soc. Am. Bull., Vol. 95, No. 8, p. 913-921.

Cavanaugh, B. J., 1979. Rb/Sr Geochronology of Some Pre-Nubian Igneous Complexes of Central and Northeastern Sudan, Unpublished Ph.D. thesis, University of Leeds.

Chavez, P.S., Jr., Guptill, S.C., and Bowell, J.A., 1984. Image Processing Techniques fo Thematic Mapper Data, Proc. Amer. Soc. of Photogrammetry Conf., Wash., D.C.

Chevremont, P., and Johan, Z., 1981. Complexe Intrusif Stratifie de Wadi Kamal-Wadi Murattiyah (Arabie Saoudite), Son Evolution Magmatique et Metallogenique: BRGM (France), Section II, Geologie des Gites Mineraux, Number 2, p. 21-40.

Cobbing, E. J., 1978, The Andean Geosyncline in Peru, and its Distinction from Alpine Geosynclines; Journal Geological Society London, Vol. 135, p. 207-218.

C

Connor, K. 1982. The Mineral Industry of Sudan: Minerals Yearbook, p. 845-850.

Conway, C. M., Elliott, J. E. and Stoesser, D., 1979. Mineral Belt Studies: U.S. Geological Survey, Prof. Paper 1150, 332 p.

Cortial, P., Lefevre, J. C. and Salih, H. M., 1986. Gold Deposits Related to the Volcano Sedimentary Sequence of Ariab, Sudan, In Prospecting In Areas of Desert Terrain, London, The Institution of Mining and Metallurgy, p. 155-159.

Coulomb, J. J., Felenc, J., and Testard, J., 1981. Volcanism et Mineralisations a Zn-Cu de la Ceinture d'Al Amar (Royaume d'Arabie Saoudite): BRGM (France), Section II, Geologie des Gites Mineraux, Number 2, p. 41-72.

D

Davies, F. B., 1984. Strain Analysis of Wrench Faults and Collision Tectonics of the Arabian-Nubian Shield, Journal Geol., Vol. 92, No. 1, P. 37-53.

Dawoud, A.S., 1982. Mozambiquan and Pan-African Events in Part of the Nubian Shield, North Nile Province, Sudan, Univ. Khartoum, Khartoum, SUDAN.

Dayuerman, H. J. and others, 1982. Late Proterozoic Evolution of Afro-Arabian Crust from Ocean Arc to Craton, Discussion and Reply, Geol. Soc. Am. Bull., Vol. 93, No. 2, p. 174-178.

Delfour, J., 1976. Comparative Study of Mineralization in the Nubian and Arabian Shields, DGMR Mineral Resources Bulletin 15, 22 p.

Delfour, J., 1981. Geologic, Tectonic and Metallogenic Evolution of the Northern Part of the Precambrian Arabian Shield: BRGM (France) Section II, Geologie des Gites Mineraux, Number 2, p. 1-20.

Dodge, F.C.W., and Rossman, D.L., 1975. Mineralization in the Wadi Qatan Area, Kingdom of Saudi Arabia, U.S. Geological Survey Saudi Arabian Project Report 190, 71 p.

Drysdall, A. R., Ramsay, C. R., and Stoeser, D. B., eds., 1986. Felsic Plutonic Rocks and Associated Mineralization of the Kingdom of Saudi Arabia, Journal of African Earth Sciences, Special Volume, Vol. 4.

E

El Boushi, I. M., 1972. Geology of the Gebeit Gold Mine, Democratic Republic of Sudan, Economic Geology, Vol. 67, No. 4, p. 481-486.

El-Gaby, S., 1985. On the Relation Between Tectonics and Ore Mineral Occurrences in the Basement Complex of the Eastern Desert of Egypt, International Conference on Basement Tectonics, 1985, Sante Fe, New Mexico, Proceedings, 26 p.

El Ghawaby, M. A., 1981, Role of Structural Deformation in Controlling Copper Occurrences in Abu Swayel Region, Egypt. International Basement Tectonics Association Publication No. 4, p. 165-172.

EL-Nadi, A. H., 1984. The Geology of the Late Precambrian Metavolcanics, Red Sea Hills, Northeast Sudan, University of Nottingham, PhD. Thesis, 245 p.

El Ramly, M. F., 1972. A New Geological Map of the Basement Rocks in the Eastern and Southwestern Deserts of Egypt, Geol. Survey Egypt Annals, Vol. 2, p. 1-18, Scale 1:1000,000.

El Shazly, E. M., Hashad, A. H., Sayyah, T. A., and Bassyuni, F. A., 1973. Geochronology of Abu Swayel Area, South Eastern Desert, Egypt, Journal of Geology Vol. 17, No. 1, p. 1-18.

El Shazly, E. M., El Sokkay, A. A., and Aly M. M., 1982. Development of Granitics and Associated Granitoids in Egypt According to Alternative Orogenic and Plate Tectonic Models, Precambrian Res., Vol. 16, No. 4, p. A56.

Embleton, J. C. B., Hughes, D. J., Klemenic, P. M., Poole, S. and Vail, J. R., 1982. A New Approach to The Stratigraphy and Tectonic Evolution of the Red Sea Hills, Sudan, Precambrian Research, Vol. 16, No. 4, p. A19 (Abs.).

Engel, A. E. J., Dixon T. H., and Stern, R. J., 1980. Late Precambrian Evolution of Afro-Arabian Crust from Ocean Arc to Craton, Geological Soc. of Am. Bull. Part I, Vol. 91, p. 699-706.

F

Fitches, W. R., Graham, R. M., Hussein, I. M., Ries, A. C., Shackleton, R. M., and Price, R. C., 1983. The Late Proterozoic Ophiolite of Sol Hamed, N.E. SUDAN, Precambrian Research, Vol. 19, p. 385-411.

Fleck, R. J., Coleman, R. G., Cornwall, H. R., Greenwood, W. R., Hadley, D. G., Schmidt, D. L., Prinz, W. C. and Ratte, J. C., 1976. Geochronology of the Arabian Shield, Western Saudi Arabia: K-Ar Results, Geological Soc. Amer. Bulletin, Vol. 87, p. 9-21.

Fleck, R. J. and others, 1981. Geochronology and Isotope Studies, U.S. Geological Surv., Prof. Paper 1275, 291 p.

G

Gabert, V. G., Ruxton, B. P. and Venzlaff, H., 1960. Uber Untersuchungen in Kristallin der Nordlichen Red Sea Hills in Sudan, Geologisches Jahrbuch, Band 77, p. 241-270.

Garson, M. S., and Miroslav, K. R. S., 1976. Geophysical and Geological Evidence of the Relationship of Red Sea Transverse Tectonics to Ancient Fractures, Geological Society of America, Bulletin, Vol. 87, p. 169-181.

Garson, M. S., and Shalaby, I. M., 1976. Precambrian-Lower Paleozoic Plate Tectonics and Metallogenesis in the Red Sea Region, Geol. Assoc. of Canada, Special Paper No. 14, p. 573-595.

Gaskell, J. L., 1985. Reappraisal of Gebeit Gold Mine, Northeast Sudan: A Case History, in Prospecting in Areas of Desert Terrain, The Institution of Mining and Metallurgy, p. 49-58.

Gass, I. G., 1979. Evolutionary Model for the Pan-African Crystalline Basement, in Al-Shanti, A.M.S., (ed.), Evolution and Mineralisation of the Arabian-Nubian Shelf, Vol. 1, King Abdul Aziz Univ., Inst. Appl. Geol. Bull. 3, Permagon Press, Oxford and New York, p. 11-20.

Gass, I.G., 1982. Upper Proterozoic (Pan-African) Calc-Alkaline Magmatism in North-Eastern Africa and Arabia, in Thorpe, R.S., ed., Andesites, Orogenic Andesites and Related Rocks, Chichester, John Wiley and Sons, p. 591-609.

G

Greenberg, J. K., 1981. Characteristics and Origin of Egyptian Younger Granites, Summary, Geol. Soc. of Amer. Bull., Part I, Vol. 92, p. 224-232.

Greiling, R., Kroner, A., and El Ramly, M. F., 1984. Structural Interference Patterns and Their Origin in the Pan-African Basement of the Southeastern Desert of Egypt, in Kroner, A., Grielins, R., editors, Precambrian Tectonics Illustrated, Federal Republic of Germany, E. Schweizer bartlsche Verlags-buchhandl, p. 401-412.

Greenwood, W. R., Anderson, R. E., Fleck, R. J., and Roberts, R. J., 1980. Precambrian Geologic History and Plate Tectonic Evolution of the Arabian Shield, DGMR Mineral Resources Bulletin 24, 35 p.

Greenwood, W. R. and Brown, G. F., 1973. Petrology and Chemical Analyses of Selected Plutonic Rocks from the Arabian Shield, Kingdom of Saudi Arabia: DGMR Mineral Resources Bulletin 9, 9 p.

Greenwood, W. R., Hadley, D. G., Anderson, R. E., Fleck, R. J., and Schmidt, D. L., 1976. Late Proterozoic Cratonization in Southwestern Saudi Arabia: Royal Society London Philos. Trans., A,, Vol. 280, p. 517-527.

H

Harris, N.B.W., 1982. The Petrogenesis of Alkaline Intrusives from Arabia and Northeast Africa and Their Implications for Within-plate Magmatism, Tectonophysics, Vol. 83, p. 243-258.

Harris, N. B., Hawkeswoth, C. J. and Ries, A. C., 1984. Crustal Evolution in Northeast and East Africa from Modal Nb Ages, Nature, Vol. 309, p. 773-776.

Hepworth, J. V., 1979. Does the Mozambique Orogenic Belt Continue into Saudi Arabia?, in Al-Shanti, A. M. S. (ed.), Evolution and Mineralisation of the Arabian-Nubian Shield, Vol. 1, King Abdul Aziz Univ., Inst. Appl. Geol. Bull. 3, Pergamon Press Oxford - New York, p. 39-51.

Hollister, L. S., and Crawford, M. L., 1986. Melt-Enhanced Deformation; A Major Tectonic Process, Geology, Vol. 14, No. 7, p. 558-561.

Hord, R.M., 1982. Digital Processing of Remotely Sensed Data. Academic Press.

H

Hussein, I.M., Kroner, A., and St. Dorr, 1982. Wadi Onib: A Dismembered Pan-African Ophiolite in the Red Sea Hills of the Sudan, Precambrian Research, Vol. 16, p. 452.

I

Ishag, A. H., 1980. A Guide to Mineral Investment In The Sudan: Democratic Republic of Sudan, Ministry of Energy and Mining, Geological and Mineral Resources Department, Bull. No. 31, 25 p.

J

Jackaman, B. 1972. Genetic and Environmental Factors Controlling the Formation of the Massive Suplhide Deposits of Wadi Bidah and Wadi Wassat, Saudi Arabia, Tech. Report TR-1972-1, Director General of Mineral Resources, Ministry of Petroleum and Mineral Resources, 243 p.

K

Kabesh, M. L., 1964. Classification of the Mineral Deposits of the Sudan, Jour. Geology U. A. R., Vol. 8. No. 2, p. 53-66.

Kabesh and Afia (1959). The Wollastonill Deposit of Dirbat Well, Bull. Geol. Surv. Sudan, No. 5. 32 pp.

Kabesh, M. L., 1961. The Geology and Economic Minerals and Rocks of the Ingessana Hills, Republic of the Sudan, Republic of the Sudan, Ministry of Mineral Resources, Geological Survey Department, Bull. No. 11, 61 p.

Kabesh, M. L., 1962. The Geology of Muhammad Qol Sheet: Sudan Geological Survey Department, Memoir No. 3.

Kabesh, M. L., Afia, M. S., and Widatalla, A. L., 1958. Fodikwan Iron Deposits, Dungunab District, North Eastern Red Sea Hills, Sudan Survey Department., Bull. No. 4, 29 p.

Kazmin, V., 1978. Geology of the Ethopian Basement and Possible Relation Between the Mozambique and Red Sea Belts: Egypt. Journal Geology, Vol. 22, No. 1.

Kroner, A., and Jahn, B. M., 1985. Precambrian Crustal Evolution, Precambrian Res., Vol. 27, p. 277-300.

K

Kroner, A., 1985. Ophiolites and the Evolution of Tectonic Boundaries in the Late Proterozoic Arabian - Nubian Shield of Northeast Africa and Arabia. Precambrian Research, Vol. 27, p. 277-300.

Kroner, A., 1979. Pan-African Mobile Belts as Evidence for a Transitional Tectonic Regime from Intraplate Orogeny to Plate Margin Orogeny, Inst. of Appl. Geology Bull. No. 3, King Abdul Aziz Univ., Jeddah, Kingdom of Saudia Arabia, Evolution and Mineralization of the Arabian-Nubian Shield, p. 21-37.

L

Lillesand, T. M. and Kiefer, R. W., 1979. Remote Sensing and Image Interpretation, John Wiley and Sons, New York, 612 p.

Lyon, R. J. P., 1981. Status of Remote Sensing Technology in Exploration, Stanford Remote Sensing Laboratory Tech. Rpt. 81-11, 12 p.

M

Merembeck, B.F., Borden, F.Y., Podwysocki, M.H., Applegate, D.N., 1976. Application of Canonical Analysis to Multispectral Scanner Data., Proc. 14th Ann. Symposium on Computer Applications in the Mineral industries, Pennsylvania, September 1976.

Moore, J. M., 1982. Structure, Stratigraphy, and Mineralization in the Southern Arabian Shield: A Study in Satellite - Image Interpretations, Precambrian Res., Vol. 16, No. 4, p. A53-A54.

N

Nagy, R. M., Ghuma M., and Rogers, J. J. W., 1976. A Crustal Suture and Lineament in North Africa, Tectonophysics, Vol. 31, No. 3-4, p. T67-T72.

Neary, C. R. 1978. Evolution and Mineralization of the Arabian - Nubian Shields, Mining Mag., Vol. 143, No. 7, p. 47-48.

Neary, C. R., Gass, I. G., and Cavanaugh, B. J., 1976. Granitic Association of Northeastern Sudan, Geol. Society of America Bull., Vol. 87, p. 1501-1512.

O

Overstreet, W.C. and Rossman, D.L., 1970. Reconnaissance Geology of the Wadi Wassat Quadrangle, Kingdom of Saudi Arabia, U.S. Geological Survey Saudi Arabian Project Report 117, 69 p.

P

Podwysocki, M. H., Gunther F.J., and Blodget, H.W., 1977. Discrimination of Rock and Soil Types by Digital Analysis of Landsat Data, NASA TM X-71290, 37 p.

Powell, C. M., 1984. Terminal Fold-Belt Deformation: Relationship of Mid-Carboniferous Mega Kinks in the Tasman Fold Belt to Coeval Thrusts in Cratonic Australia, Geology Vol. 12, p. 546-549.

R

Ressetar, R., and Monrad, J. R., 1983. Chemical Composition and Tectonic Setting of the Dokhan Volcanic Formation, Eastern Desert, Egypt, Journal of African Earth Sciences, Vol. 1, No. 2, p. 103-112.

Reymer, A. P. S., 1984. Metamorphism and Tectonics of a Pan-African Terrain in Southeastern Sinai; A Reply, Precambrian Res., Vol. 24, No. 2, p. 189-197.

Reymer, A. P. S., 1983. Metamorphism and Tectonics of a Pan-African Terrain in Southeastern Sinai. Precambrian Research, Vol. 19, p. 225-238.

Ries, A.C., Shackleton, R.M., Graham, R.M., and Fitches, W. R., 1983. Pan-African Structures, Ophiolites and Melanges in the Eastern Desert of Egypt: A Traverse at 26°N, Journal Geol. Soc. London, Vol. 140, p. 75-95.

Routhier, P., and Delfour, J., 1980. Geology of Massive Sulfide Deposits Associated with Acid Volcanism and its Application to the Search for Such Deposits in the Precambrian of Saudi Arabia, DGMR Mineral Resources Bulletin 18, 61 p.

Rowan, L. C., Wetlaufer, P. H., Goetz, A. F. H., Billingsley, F. C., and Stewart, J. H., 1976. Discrimination of Rock Types and Detection of Hydrothermally Altered Areas in South-Central Nevada by the Use of Computer-Enhanced ERTS Images, U. S. Geol. Survey Prof. Paper 883, 35 p.

R

Ruxton, B. P., 1956. The Major Rock Groups of the Northern Red Sea Hills, Sudan, Geology Mag., Vol. 93, No. 4, p. 314-331.

S

Sabert, A. M. 1981. Tectonics of the Northern Red Sea Hills, Proc. of the 4th Intl. Conf. on Basement Tectonics, p. 201-208.

Sabir, H., 1981. Metallogenic and Textural Features of Sulfide Mineralization at Jabal Sayid, Saudi Arabia: BRGM (France) Section II, Geologie des Gites Mineraux, Number 2, p. 103-111.

Said, R., 1962. The Geology of Egypt, Elsevier Publishing Co., Amsterdam.

Salama, R.B., 1985. Buried Troughs, Grabens and Rifts in Sudan, Journal of African Earth Sciences, Vol. 3, No. 3, P. 381-390.

Schmidt, D. L., Hadley, D. G., and Stoeser, D. B., 1979. Late Protezoroic Crustal History of the Arabian Shield, Southern Najd Province, Kingdom of Saudi Arabia: in "Evolution and Mineralization of the Arabian-Nubian Shield", Inst. App. Geology Bulletin 3, Vol. 2, p. 41-58.

Serencsits, C. McC., Faul, H., Foland, K.A., Hussein, A.A., and Lutz, T.M., 1981. Alkaline Ring Complexes in Egypt: Their Ages and Relationship in Time, Journal of Geophysical Research, Vol. 86, No. B4, p. 3009-3013.

Sestini, J., 1965. Cenozoic Stratigraphy and Depositional History, Red Sea Coast, Sudan, Bull. of Amer. Assoc. of Pet. Geol., Vol. 49, No. 9, p. 1453-1472.

Shackleton, R. M., Ries, A. C., Graham, R. H., and Fitches,
W. R., 1980. Late Precambrian Ophiolitic Melange in the Eastern Desert of Egypt, Nature, Vol. 285, p. 472-474.

Shackleton, R. M., 1986. Precambrian Collision Tectonics in Africa, in Coward, M. P., and Ries, A. C., (eds), Collision Tectonics, Geological Society Special Publication No. 19, p. 329-349.

Shaddad, M. Z., 1978. Sudan: Mining Annual Review, p. 514-515.

S

Sheffield, C., 1985. Selecting Band Combinations from Multispectral Data, Photogrammetric Engineering and Remote Sensing, Vol. 51, No. 6, p. 681-687.

Shekarchi, E., 1978-79. The Mineral Industry of Sudan, Minerals Yearbook, Vol. 3, p. 867-872.

Shimron, A. E., 1984. Evolution of the Kid Group, Southeast Sinai Peninsula: Thrusts, Melanges, and Implications for Accretionary Tectonics During the Late Proterozoic of the Arabian-Nubian Shield, Geology, Vol. 12, p. 242-247.

Sillitoe, R. M., 1979. Metallogenic Consequences of Late Precambrian Suturing in Arabia, Egypt, Sudan and Iran, Instit. of Appl. Geol. (I.A.G. Bulletin #3); King Abdul Aziz Univ., Jeddah, Kingdom of Saudi Arabia, Evolution and Mineralization of the Arabian-Nubian Shield. p. 110-120.

Soliman, M. M., 1981. Mineral Exploration in Egypt, Proc. of the 4th Intl. Conf. on Basement Tectonics, Oslo, Norway, p. 157-163.

Stacey, J. S., and Hedge, C. E., 1984. Geochronologic and Isotope Evidence for Early Proterozoic Crust in the Eastern Arabian Shield, Geology, Vol. 12, p. 310-313.

Stacey, J. S., and Stoeser, D. B., 1983. Distribution of Oceanic and Continental Leads in the Arabian-Nubian Shield, Contrib. to Mineralogy and Petrology Vol. 84, p. 91-105.

Stern, R. J., 1982. Petrogenesis and Tectonic Setting of Late Precambrian Ensimatic Volcanic Rocks, Central Eastern Desert of Egypt, Precambrian Research, Vol. 16, p. 195-230.

Stern, R. J., Gottfield, D., and Hedge, C.E., 1984. Late Precambrian Rifting and Crustal Evolution in the Northeastern Desert of Egypt, Geology, Vol. 12, p. 168-172.

Stern, R. J., and Hedge C. E., 1985. Geochronologic and Isotopic Constraints on Late Precambrian Crustal Evolution in the Eastern Desert of Egypt, Am. Jour. Sci., Vol. 285, No. 2, p. 97-127.

S

Stoeser, D. B., Stacey, J.S., Greenwood, W.R., and Fisher, L.B., 1984. U/Pb Zircon Geochronology of the Southern Part of the Nabitah Mobile Belt and Pan-African Continental Collision in the Saudi Arabian Shield, U.S. Geol. Surv., Open-File Report, 92 p.

Stoeser, D. B., and Camp, V. E., 1985. Pan-African Microplate Accretion of the Arabian Shield, Geol. Soc. of America Bulletin, Vol. 96, p. 817-826.

Stoeser, D. B., and Stacey, J. S., 1983. Granitoid Plutonic Rocks of the Arabian Shield, U.S. Geol. Surv., Prof. Paper 1375, 287 p.

Sturchio, N. C., 1983. Geologic Evolution of Precambrian Basement of Eastern Desert of Egypt, AAPG Bulletin, Vol. 67, No. 3, p. 554.

Sturchio, N. C., Sultan, M., and Batiza, R., 1983. Geology and Origin of Meatig Dane, Egypt: A Precambrian Metamorphic Core Complex?, Geology, Vol. 11., p. 72-76.

T

Taylor, M.M., 1974. Principal Components Color Display of ERTS Imagery, Third Earth Resources Technology Satellite Symp., Washington, D.C., Section B.

Technoexport, 1974. Results of K-Ar Absolute Age Determination. Report by Ministry of Geology of the U.S.S.R. for the Sudan Government, Report of the Geological Survey of Sudan, Unpublished.

V

Vail, J. R., 1985. Pan-African (late Precambrian) Tectonic Terrains and the Reconstruction of the Arabian-Nubian Shield, Geology, Vol. 13, p. 839-842.

Vail, J. R., 1984. The Nature of the Basement Complex of the Nubian Shield in North-east Africa: Addendum, Journal of African Earth Sciences, Vol. 2, No. 4, p. 389-390.

Vail, J. R., 1983. Pan-African Crustal Accretion in North-east Africa, Journal of African Earth Sciences, Vol. 1, No. 3/4, pp. 285-294.

V

Vail, J. R., 1979. Outline of Geology and Mineralization of the Nubian Shield East of the Nile Valley, Sudan: in Al-Shanti, A.M.S. (ed.), Evolution and Mineralization of the Arabian-Nubian Shield, Vol. 1, King Abdul Aziz Univ., Inst. Appl. Geol. Bull. 3, Pergamon Press, Oxford - New York, p. 97-107.

Vail, J. R., 1978. Outline of the Geology and Mineral Deposits of the Democratic Republic of the Sudan and Adjacent Areas, Overseas Geology and Mineral Resources, No. 49, Inst. of Geolog. Sciences, London.

Warden, A. J., 1982. The Northeast Branch of the Mozambique Belt, Precambran Res., Vol. 16, No. 4, p. A41-A42.

Weissenborn, A. E., and Earhart, R.L., 1968. Appraisal of the Wadi Wassat and Wadi Abhat Pyrite Deposits, Asir Quadrangle, Kingdom of Saudi Arabia, U.S. Geological Survey Saudi Arabian Project Tech. Letter 101, 21 p.

Whiteman, A. J., 1971. The Geology of the Sudan Republic, Oxford, Clarendon Press, XIV, 290 p.

Woodward, L. A., 1984. Basement Control of Tertiary Intrusions and Associated Mineral Deposits Along Tijeras - Canoncito Fault System, New Mexico, Geology, Vol. 12, p. 531-533.